



Article

Powders Synthesized from Calcium Chloride and Mixed-Anionic Solution Containing Orthophosphate and Carbonate Ions

Tatiana V. Safronova ^{1,2},*, Hieu Minh Ngoc Le ¹, Tatiana B. Shatalova ^{1,2}, Albina M. Murashko ², Tatiana V. Filippova ¹, Egor A. Motorin ², Dmitry M. Tsymbarenko ¹, Daniil O. Golubchikov ², Olga V. Boytsova ^{1,2} and Alexander V. Knotko ²

- Department of Chemistry, Lomonosov Moscow State University, Building, 3, Leninskie Gory, 1, 119991 Moscow, Russia; lengokmin@my.msu.ru (H.M.N.L.); shatalovatb@my.msu.ru (T.B.S.); tania.filippova@inorg.chem.msu.ru (T.V.F.); tsymbarenko@gmail.com (D.M.T.); boytsovaov@my.msu.ru (O.V.B.)
- Department of Materials Science, Lomonosov Moscow State University, Building, 73, Leninskie Gory, 1, 119991 Moscow, Russia; murashkoam@my.msu.ru (A.M.M.); motorinea@my.msu.ru (E.A.M.); golubchikovdo@my.msu.ru (D.O.G.); alknt@mail.ru (A.V.K.)
- * Correspondence: safronovatv@my.msu.ru; Tel.: +7-(916)-3470641

Abstract

Low-crystalline hydroxyapatite was synthesized from an aqueous solution of calcium chloride (CaCl₂), and a mixed-anionic (HPO₄²⁻ u CO₃²⁻) aqueous solution prepared from potassium hydrophosphate trihydrate (K₂HPO₄·3H₂O), and potassium carbonate (K₂CO₃). The interaction of K₂CO₃ and K₂HPO₄ salts during synthesis from a mixedanionic solution in the reaction zone without additional regulation provided the pH level necessary for the synthesis of hydroxyapatite. For comparison, as references, powders were also synthesized from an aqueous solution of CaCl2 and from aqueous solutions of either K₂HPO₄ or K₂CO₃. The phase composition of the powder synthesized from aqueous solutions of CaCl₂ and K₂HPO₄ included brushite (CaHPO₄·2H₂O). The phase composition of the powder synthesized from aqueous solutions of CaCl₂ and K₂CO₃ included calcite (CaCO₃). The phase composition of all synthesized powders contained potassium chloride (sylvine, KCl), as a reaction by-product. After heat treatment at 1000 °C of the powder containing low-crystalline hydroxyapatite and KCl, powder of chlorapatite (Ca₁₀(PO₄)₆Cl₂) was obtained. After heat treatment of a powder containing brushite (CaHPO₄·2H₂O) and KCl at 800 and 1000 $^{\circ}$ C, a powder with the phase composition including β -calcium pyrophosphate (β-Ca₂P₂O₇), β-calcium orthophosphate (β-Ca₃(PO₄)₂), and potassiumcalcium pyrophosphate (K₂CaP₂O₇) was obtained. Heat treatment of calcite (CaCO₃) powder at 800 °C, as expected, led to the formation of calcium oxide (CaO). Synthesized powders, including biocompatible minerals such as hydroxyapatite, chlorapatite, brushite, monetite, calcium pyrophosphate, calcium potassium pyrophosphate, tricalcium phosphate, and calcite, can be used for the creation of biocompatible inorganic materials or composite materials with a biocompatible polymer matrix. The potassium chloride present in the synthesized powders can act as one of the precursors of biocompatible minerals, such as chlorapatite or calcium potassium pyrophosphate, or it can be treated as a removable inorganic porogen.

Keywords: synthesis; mixed-anionic solution; hydroxyapatite; brushite; calcite; sylvine; monetite; calcium pyrophosphate; tricalcium phosphate; calcium potassium pyrophosphate; chlorapatite



Academic Editor: Franco Bisceglie

Received: 24 August 2025 Revised: 27 September 2025 Accepted: 11 October 2025 Published: 15 October 2025

Citation: Safronova, T.V.; Le, H.M.N.; Shatalova, T.B.; Murashko, A.M.; Filippova, T.V.; Motorin, E.A.; Tsymbarenko, D.M.; Golubchikov, D.O.; Boytsova, O.V.; Knotko, A.V. Powders Synthesized from Calcium Chloride and Mixed-Anionic Solution Containing Orthophosphate and Carbonate Ions. *Compounds* 2025, 5, 41. https://doi.org/10.3390/compounds5040041

Copyright: © 2025 by the authors.
Licensee MDPI, Basel, Switzerland.
This article is an open access article distributed under the terms and conditions of the Creative Commons Attribution (CC BY) license (https://creativecommons.org/licenses/by/4.0/).

Compounds **2025**, 5, 41 2 of 23

1. Introduction

Fine powders with a given chemical and phase composition and high uniformity of component distribution are required for the creation of inorganic materials or composite materials with unique functional properties [1–3]. The simplest and most obvious is the method of mechanical homogenization of powder mixtures, which is carried out using special equipment, such as a planetary mill [4]. High-temperature solid-phase synthesis from a homogeneous mixture of salts obtained by drying a solution of these salts at subzero temperatures is more difficult for implementation [5]. The maximum level of homogenization is achieved in mixed-anionic compounds, which are produced using high-temperature and low-temperature reactions [6]. High-temperature reactions for the preparation of mixed-anionic compounds can take place during synthesis in the solid phase, in synthesis by interaction of gas and solid phases, and synthesis in conditions using pressure. Low-temperature reactions for the preparation of mixed-anionic compounds can take place in topochemical synthesis, solvothermal synthesis, and synthesis in thin films. Precipitation of hydroxides [7], carbonates, or oxalates is also used to obtain homogeneous precursors of oxide powders [8]. Synthesis of inorganic powders consisting of small particles with a high specific surface area and activity via precipitation from solution is the most convenient for implementation [9].

High uniformity of the distribution of components in a powder intended for the production of biocompatible materials can be achieved using synthesis from both mixed-cationic [10] and mixed-anionic solutions, for example, containing HPO₄²⁻/P₂O₇⁴⁻ [11], HPO₄²⁻/CO₃²⁻ [12–14], P₂O₇⁴⁻/CO₃²⁻ [15], HPO₄²⁻/SiO₃²⁻ [16], and HPO₄²⁻/SO₄²⁻ [17]. High uniformity of the distribution of components in powder can be reached in case of similarity of crystal structures of minerals, for example, brushite (CaHPO₄·2H₂O), gypsum (CaSO₄·2H₂O), and ardealite (Ca(HPO₄)_x(SO₄)_{1-x}·2H₂O) [17]. In previous investigations, it was shown that the simultaneous presence of different anions (HPO₄²⁻/CO₃²⁻ [12], P₂O₇⁴⁻/CO₃²⁻ [15], and HPO₄²⁻/SiO₃²⁻ [16]) in the reaction zone causes the formation of a quasi-amorphous phase. And this phenomenon can be not only a sign of high uniformity of the distribution of components but also a sign of the presence of defects in the crystal lattice of the precipitated minerals, which then can provide high activity of the synthesized powders in sintering or in chemical interaction.

The mineral component of bone tissue is mainly represented by carbonate-substituted hydroxyapatite [18]. Calcium hydroxyapatite ($Ca_{10}(PO_4)_6(OH)_2$) is a well-known and unique ion exchanger [19–21]; therefore, various cations such as Na⁺, K⁺, Mg²⁺, Zn²⁺, Ba²⁺, or Sr²⁺ [22] and anions such as CO_3^{2-} or SiO_4^{4-} , F⁻, or Cl^- can be included in the composition of bone tissue [23,24].

Various powders obtained by one of the methods of chemical synthesis are used for the manufacture of bone implants, both based on calcium phosphates [25–28] and calcium carbonates [29–31]. Precipitation from solutions including a hydrophosphate ion, a carbonate ion, and a calcium ion is preferable due to the possibility of obtaining powders similar in chemical and phase composition to natural bone tissue [12–14,32]. Powders of calcium phosphates with a molar ratio Ca/P < 1.67 and calcium carbonates are used to create materials for temporary bone implants. At the same time, hydroxyapatite-based materials (molar ratio Ca/P = 1.67) are resistant to dissolution and can be used as implants for long-term substitution [33].

Materials based on calcium carbonates [34–36] and calcium phosphates with a molar ratio of Ca/P < 1.67 [37,38] are able to dissolve gradually during implantation, and, therefore, they are used in regenerative methods of bone defect treatment [39]. Synthetic powders of calcium carbonate (CaCO₃), and calcium phosphates with a molar ratio of Ca/P < 1.67 can be used as fillers in biocompatible and biodegradable composites with

Compounds 2025, 5, 41 3 of 23

polymer [40] or mineral (obtained as a result of chemical bonding reactions) matrices [41]. In addition, these powders can also be used to produce biocompatible ceramic materials, with the phase composition belonging to oxide systems, including calcium oxide and phosphorus oxide [42].

The aim of the present work consisted of preparing and investigating powders synthesized from an aqueous solution of calcium chloride (CaCl₂), and a mixed-anionic solution containing orthophosphate and carbonate ions. Potassium hydroorthophosphate (K₂HPO₄), was used as the source of orthophosphate ions, and potassium carbonate (K₂CO₃), was used as the source of carbonate ions. For comparison, as references, powders were also synthesized from an aqueous solution of calcium chloride (CaCl₂), and aqueous solutions including either potassium hydrophosphate (K₂HPO₄), or potassium carbonate (K₂CO₃). Synthesis from aqua solution of CaCl₂ and a mixed-anionic solution containing orthophosphate and carbonate ions can provide the preparation of a powder of high quality as a starting point for the creation of different biocompatible materials and materials with other specific properties. To the best of our knowledge, synthesis from a mixed-anionic solution containing K₂HPO₄ and K₂CO₃ and an aqua solution of CaCl₂ has not been considered in the scientific literature.

2. Materials and Methods

For the synthesis of powders, calcium chloride (CaCl₂) (CAS No. 10043-52-4, analytical pure grade, Rushim, Moscow, Russia), potassium hydrophosphate trihydrate ($K_2HPO_4\cdot 3H_2O$) (CAS No. 16788-57-1, analytical pure grade, Rushim, Moscow, Russia), and potassium carbonate (K_2CO_3) (CAS No. 584-08-7, chemical pure grade, Rushim, Moscow, Russia), were used.

The following reactions were used to calculate the amounts of starting salts and expected products:

$$CaCl2 + K2HPO4·3H2O \rightarrow CaHPO4·2H2O + 2KCl + H2O$$
 (1)

$$CaCl_2 + 0.5K_2HPO_4 \cdot 3H_2O + 0.5K_2CO_3 \rightarrow 0.5CaCO_3 + 0.5CaHPO_4 \cdot 2H_2O + 2KCl + 0.5H_2O \qquad (2)$$

$$CaCl2 + K2CO3 \rightarrow CaCO3 + 2KCl$$
 (3)

The labeling and synthesis conditions of the powders from $CaCl_2$ and K_2HPO_4 and/or K_2CO_3 are shown in Table 1.

Table 1. The labeling and synthesis conditions of the powders.

Labeling of Powders	PO4	PO4_CO3	CO3
The molar ratio of $Ca/(HPO_4^{2-} + CO_3^{2-})$	1	1	1
CaCl ₂ , mol	0.25	0.25	0.25
V of solution CaCl ₂ , L	0.5	0.5	0.5
C (CaCl ₂), mol/L	0.5	0.5	0.5
$K_2HPO_4 \cdot 3H_2O$, mol	0.25	0.125	-
K_2CO_3 , моль	-	0.125	0.25
V of solution, containing anions (HPO ₄ ²⁻) and/or (CO ₃ ²⁻), L	0.5	0.5	0.5
$C(K_2HPO_4\cdot 3H_2O)$, mol/L	0.5	0.25	-
$C(K_2CO_3)$, mol/L	-	0.25	0.5

A total of 500 mL of 0.5 M aqueous solution of K_2HPO_4 (PO4 powder), 500 mL of 0.5 M aqueous solution of K_2CO_3 (CO3 powder), 500 mL aqueous solution containing 0.125 M of K_2HPO_4 , and 0.125 M of K_2CO_3 (PO4_CO3 powder) were added to 500 mL of 0.5 M aqueous CaCl₂ solutions. The resulting suspensions were kept on a stirrer (MAG C Hs7 IKA

Compounds 2025, 5, 41 4 of 23

(IKA-Werke GmbH & Co. KG, Staufen, Germany)) for 30 min. The resulting precipitates were separated from the mother liquor using vacuum filtration. The synthesized powders were dried in a thin layer at room temperature for a week. After drying, the powders were crushed using an agate mortar and pestle and then passed through a polyester sieve with a mesh size of 200 microns. For the isolation of salts dissolved in the mother liquors, they were dried at 40 °C for a month. The synthesized powders and isolated reaction by-products were weighed to determine their mass and to estimate the yield of synthesized powders and reaction by-products relative to the theoretically possible amounts. Table 2 shows the initial quantities, expected target products, and reaction by-products calculated in accordance with reactions (1–3).

Table 2. Quantities of initial reagents, as well as expected target products and reaction by-products.

Decembe/Duradurate	Labeling of Synthesized Powders			
Reagents/Products	PO4	PO4_CO3	CO3	
Starting Reagents				
CaCl ₂ , mol	0.25	0.25	0.25	
$K_2HPO_4\cdot 3H_2O$, mol	0.25	0.125	-	
K_2CO_3 , mol	-	0.125	0.25	
Target products				
$CaHPO_4 \cdot 2H_2O$, mol	0.25	0.125	-	
Mass of CaHPO ₄ ·2H ₂ O, g	43.0	21.5	-	
CaCO ₃ , mol	-	0.125	0.25	
Mass of CaCO ₃ , g	-	12.5	25.0	

By-product –	Labeling of by-products			
	PO4_by	PO4_CO3_by	CO3_by	
KCl, mol	0.5	0.5	0.5	
Mass of KCl, г	37.3	37.3	37.3	
Total mass of expected products *	80.3	73.1	62.3	

^{*} The total mass of the expected products is defined as the sum of the mass of target products (CaHPO $_4\cdot 2H_2O$ and/or CaCO $_3$) and mass of reaction by-products (KCl).

To study the thermal evolution of the phase composition of the synthesized powders, they were placed in porcelain boats and heated at a heating rate of 5 $^{\circ}$ C/min, followed by exposure for 2 h at various temperatures in the range of 200–1000 $^{\circ}$ C. The labeling of the powders after heat treatment used in the figures is shown in Table 3.

Table 3. Labeling of powders obtained after heat treatment.

Temperature of	Labe	eling of Synthesized Pow	ders
Heat Treatment	PO4	PO4_CO3	CO3
200 °C	PO4_200	PO4_CO3_200	CO3_200
400 °C	PO4_400	PO4_CO3_400	CO3_400
600 °C	PO4_600	PO4_CO3_600	CO3_600
800 °C	PO4_800	PO4_CO3_800	CO3_800
1000 °C	PO4_1000	PO4_CO3_1000	-

The phase composition of powders after synthesis and after heat treatment was performed by X-ray powder diffraction (XRD) analysis using CuKa radiation (λ = 1.5418 Å, step 20—0.02°) using Rigaku D/Max-2500 diffractometers (Rigaku Corporation, Tokyo, Japan) in the angle range 20 from 2 to 70° or Tongda TD-3700 (Dandong Tongda Science & Technology Co., Ltd., Dandong, China) in the angle range 20 from 3 to 70°. The X-ray patterns were analyzed using the WinXPOW program (Version 1.06) using the ICDD PDF-2 (https://www.icdd.com/pdf-2/, accessed on 18 August 2025) [43] databases and the

Compounds **2025**, 5, 41 5 of 23

Match! program ((Version 3.15), https://www.crystalimpact.com/, accessed on 18 August 2025). The quantitative ratio of the target and related products in the obtained powders was determined using the Match! Program ((Version 3.15), https://www.crystalimpact.com/, accessed on 18 August 2025). The infrared (IR) spectra were collected in the wavelength range 500–4000 cm⁻¹ using the Spectrum Three IR spectrometer (Perkin Elmer, Waltham, MA, USA) in the mode of disturbed total internal reflection using the Universal ATR accessory (crystal diamond/KRS-5). The bands in the spectra were assigned based on the literature data [44]. Synchronous thermal analysis (TA), including thermogravimetric analysis (TGA) and differential scanning calorimetry (DSC), was performed on a NETZSCH STA 449 F3 Jupiter thermal analyzer (NETZSCH, Selb, Germany) in air in the temperature range of 40–1000 °C at a heating rate of 10 °C/min, using pre-thermostating at 40 °C for 30 min. The mass of the sample was at least 10 mg. The composition of the gas phase was monitored using a Netzsch QMS 403 Quadro quadrupole mass spectrometer (NETZSCH, Selb, Germany) combined with a NETZSCH STA 449 F3 Jupiter thermal analyzer (NETZSCH, Selb, Germany). Mass spectra (MS) were recorded for m/z = 44 (CO₂). The microstructure of the powders was studied by scanning electron microscopy (SEM) using a scanning electron microscope with an auto emission source JEOL JSM-6000PLUS Neoscope II (JEOL Ltd., Tokyo, Japan). For the study, the samples were glued onto a copper substrate using carbon tape, and a layer of gold ~15nm was sprayed. The survey was carried out in vacuum mode. The accelerating voltage of the electron gun was up to 5 kV. The images were obtained in secondary electrons at magnifications up to 1000× and recorded in digitized form on a computer.

3. Results and Discussion

The XRD data of the synthesized powders are shown in Figure 1.

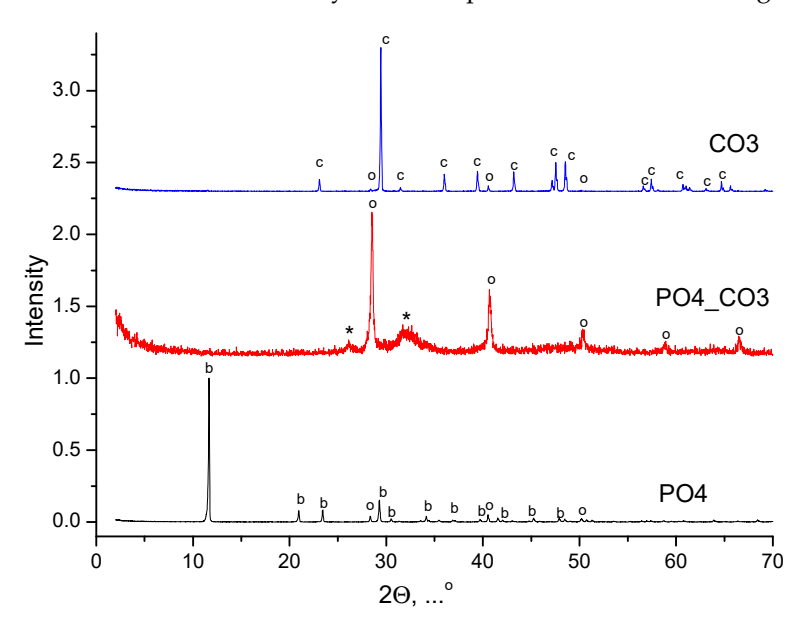


Figure 1. XRD data of synthesized powders: c—calcium carbonate (calcite, $CaCO_3$) (PDF card No 5-586; No 96-210-0190); o—potassium chloride (sylvine, KCl) (PDF card No 41-1476; No 96-900-8652); *—hydroxyapatite ($Ca_{10}(PO_4)_6(OH)_2$) (PDF card No 9-432, No 96-900-1234); b—brushite ($CaHPO_4$ · $2H_2O$) (PDF card No 9-77; No 96-231-0527).

The phase composition of powder synthesized from water solutions of $CaCl_2$ and K_2CO_3 included calcite (CaCO₃). The phase composition of powder synthesized from water solutions of $CaCl_2$ and K_2HPO_4 included brushite (CaHPO₄·2H₂O). The phase composition of powder synthesized from a water solution of $CaCl_2$ and mixed-anionic solution containing K_2CO_3 and K_2HPO_4 included a low-crystalline product with the main

Compounds 2025, 5, 41 6 of 23

peaks corresponding to hydroxyapatite $(Ca_{10}(PO_4)_6(OH)_2)$. All synthesized powders included potassium chloride (sylvine, KCl), as a reaction by-product. XRD data of reaction by-products isolated from mother liquors are presented in Figure 2. The phase composition of the by-products isolated from the mother liquors was presented by potassium chloride (sylvine, KCl).

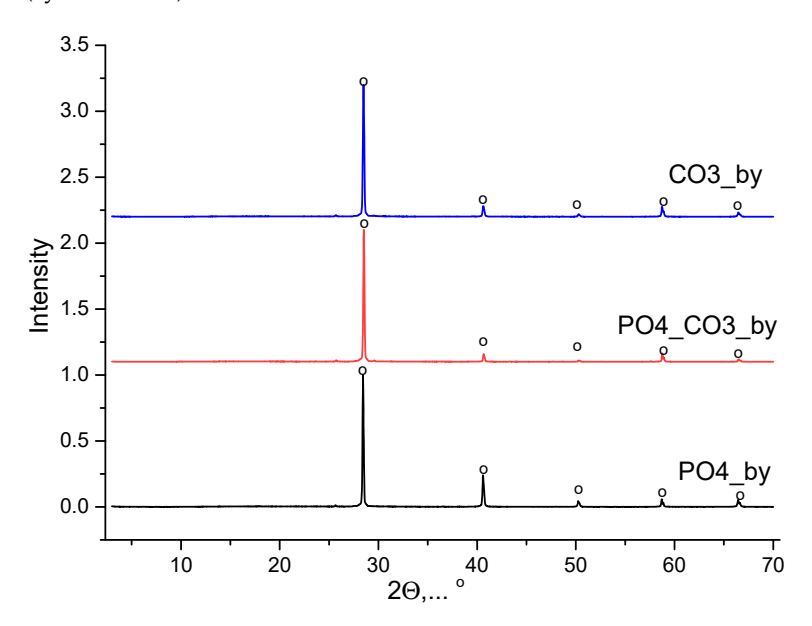


Figure 2. XRD data of products isolated from mother liquors after synthesis: o—potassium chloride (sylvine, KCl) (PDF card No 41-1476; No 96-900-8652).

It should be noted that in this investigation, the stage of reaction by-product removal from all synthesized powders via precipitate washing was not implemented. The first reason consisted of the necessity to carry out the same synthesis conditions for all powders. The second reason consisted of the intended choice of pairs of resources providing the formation of biocompatible salt (KCl) as a reaction by-product. The third reason consisted of the possibility for KCl to be used as an inorganic porogen when it is present in synthesized powders and which can be removed from created composite materials with inorganic or polymer matrices via washing. To play the role of an inorganic porogen, the substance (inorganic salt) has to be soluble in water when other constituents of materials do not have such a possibility [45–47]. KCl as a component of the starting powder mixture used for the calcium phosphate ceramics preparation can be treated as a temporary sintering additive with a low melting point, which can be removed during stage of sintering at temperatures above its melting point [48–50].

The formation of brushite (CaHPO $_4$ ·2H $_2$ O), and calcite (CaCO $_3$), can be caused by reactions (1) and (3), respectively. During the preparation of the mixed-anionic aqua solution from K_2 HPO $_4$ and K_2 CO $_3$ taken in an equimolar ratio, not only the release of CO $_2$ was observed, but also the formation of potassium orthophosphate (K_3 PO $_4$), occurred. Reaction (4) indicates that when mixing solutions of these two salts, the presence of potassium carbonate, K_2 CO $_3$, also persists.

$$2K_2HPO_4 + K_2CO_3 \rightarrow 2K_3PO_4 + H_2O + CO_2$$
 (4)

So, due to hydrolysis (reactions 5 and 6), the mixed-anionic solution had an alkaline pH, characteristic of aqua solutions of salts formed by a strong base and a weak acid:

$$K_2CO_3 + H_2O \rightarrow KHCO_3 + KOH$$
 (5)

Compounds 2025, 5, 41 7 of 23

$$K_3PO_4 + H_2O \rightarrow K_2HPO_4 + KOH$$
 (6)

The formation of a specific calcium phosphate is determined by the pH level in the reaction zone. Formation of hydroxyapatite takes place at pH > 6 in the reaction zone. The same phenomenon took place, for example, when the mixed-anionic solution of Na_2SiO_3 and Na_2HPO_4 , having an alkaline pH, interacted with a water solution of $Ca(NO_3)_2$ [51]. The synthesis of hydroxyapatite from mixed-anionic solution of K_2HPO_4 and K_2CO_3 can be represented formally as reaction (7), taking into account the molar ratio of the salts used for synthesis, as it was described in Materials and Methods (reaction 2):

$$12CaCl_2 + 6K_2HPO_4 + 6K_2CO_3 \rightarrow Ca_{10}(PO_4)_6(OH)_2 + 2CaCO_3 + 24KCl + 2H_2O + 4CO_2$$
 (7)

In this case, the theoretically possible amount of hydroxyapatite ($Ca_{10}(PO_4)_6(OH)_2$) (0.0208 mol = 20.9 g) can be calculated as 1/6 of the amount of potassium hydrophosphate (K_2HPO_4) (0.125 mol) used for preparation of a mixed-anionic solution (Table 1). Taking into account the possibility of the formation of $CaCO_3$, the mass of the precipitate can be calculated as the sum of the possible amounts of hydroxyapatite and calcium carbonate. The amount of $CaCO_3$ (0.0417 mol = 4.17 g) can be calculated as 1/6 of the amount of $CaCl_2$ (0.25 mol). Thus, the mass of the precipitate in the synthesis of $PO4_CO3$ powder can be calculated as 25.07 g. Theoretically calculated (expected) and experimentally obtained masses of target products and by-products, as well as their comparison, are presented in Table 4.

Table 4. The expected and obtained masses of synthesized powders and reaction by-products.

Labeling	PO4	PO4_CO3	CO3		
The expected quantities of	The expected quantities of target products and by-product:				
CaHPO₄·2H₂O, g	43.0	-	-		
$Ca_{10}(PO_4)_6(OH)_2 + CaCO_3, g$	-	25.1	-		
CaCO ₃ , g	-	-	25.0		
KCl, g	37.3	37.3	37.3		
Total mass of expected products *, g	80.3	62.4	62.3		
The obtained masses of the synthesiz	ed powders ar	nd the extracted b	y-products:		
Mass of the powders after drying, g	43.0	33.5	17.4		
Mass of the extracted reaction by-product, g	30.6	25.5	37.1		
Total mass of prepared products **, g	73.6	59.0	54.5		
The yield of synthesized products	91.7%	94.5%	87.5%		
The yield of reaction by-product	82.0%	68.4%	99.4%		
Mass of by-product, preserved by precipitate (estimation), g	6.7	11.8	0.2		
Content of by-product in powders (estimation)	15.6%	35.2%	1.1%		
Content of by-product in powders (estimation according to Match!)	2.8%	30.9%	1.8%		

^{*} Total mass of expected products was determined as sum of target product ($CaHPO_4 \cdot 2H_2O$ and/or $CaCO_3$) and reaction by-product (KCl). ** Total mass of prepared products was determined as sum of mass powder after drying and mass of the product extracted from the mother liquor.

The data presented in Table 4 indicate that the total yield of synthesis products was close to ~90% in all cases. According to the estimation obtained using the Match! program,

Compounds 2025, 5, 41 8 of 23

the content of the reaction by-product (KCl) was maximal (30.9%) in the powder synthesized from a mixed-anionic solution. The amount of KCl in the PO4 powder was determined as 2.8%, and in the CO3 powder, it was determined as 1.8%. The estimation of the amount of by-product in synthesized powders obtained using the Match! program is consistent with the estimation of the amount of by-product retained in PO4_CO3 and CO3 powders (Table 4). A small particle size and a significant specific surface area may determine the ability of the synthesized PO4_CO3 powder to retain (occlude) mother liquors and the by-product dissolved in it, as it has been shown in other studies [52].



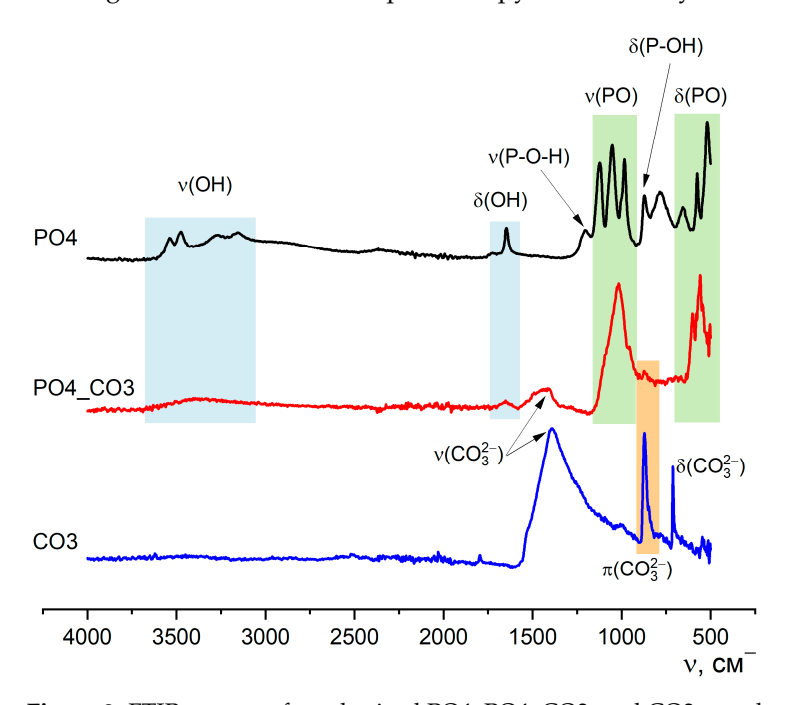


Figure 3. FTIR spectra of synthesized PO4, PO4_CO3, and CO3 powders.

The FTIR spectroscopy data (Figure 3) is consistent with the X-ray diffraction data, since the appearance of the curves corresponds to the reference and literature data for brushite (SpectraBase Spectrum ID 9u0yn3G2J6i https://spectrabase.com/spectrum/9u0 yn3G2J6i (accessed on 23 August 2025) [53–55]), calcite (SpectraBase Compound ID YYVCfbcpX1) https://spectrabase.com/compound/YYVCfbcpX1 (accessed on 23 August 2025) [56–58]), hydroxyapatite (SpectraBase Spectrum ID BxeLPnr9PTc https://spectrabase.com/spectrum/BxeLPnr9PTc (accessed on 23 August 2025) [59] and carbonate-hydroxyapatite [14,60,61]). On the spectra of PO4 and CO3 powders, there are valence (v) and deformation (δ) vibrations, which are characteristic of brushite, CaHPO₄·2H₂O: v(OH)—3539, 3473, 3270, 3153 cm⁻¹; v(P-O-H)—1204 cm⁻¹; v(PO)—1120, 1052, 980 cm⁻¹ δ (OH)—1645 cm⁻¹; 980 cm⁻¹; δ (P-OH)—871 cm⁻¹; and δ (PO)—(656, 575, 519 cm⁻¹) and calcite CaCO₃: v(CO₃²⁻)—1390 cm⁻¹; π (CO₃²⁻)—874 cm⁻¹; and δ (CO₃²⁻)—(710 cm⁻¹).

Characteristic vibrations of the phosphate group PO_4^{3-} , which confirm the formation of weakly crystallized hydroxyapatite, can also be seen on the spectrum of the PO4_CO3 powder. Vibrations of $\nu(CO_3^{2-})$ —1410 cm⁻¹ and $\pi(CO_3^{2-})$ —874 cm⁻¹ in the spectrum of PO4_CO3 powder suggest the presence of carbonate groups in the structure of the synthesized low-crystalline hydroxyapatite. The presence of KCl, regardless of its content in the synthesized powders, is not determined due to the absence of absorption bands in the studied region [62,63].

Figure 4 shows micrographs of the synthesized powders.

Compounds 2025, 5, 41 9 of 23

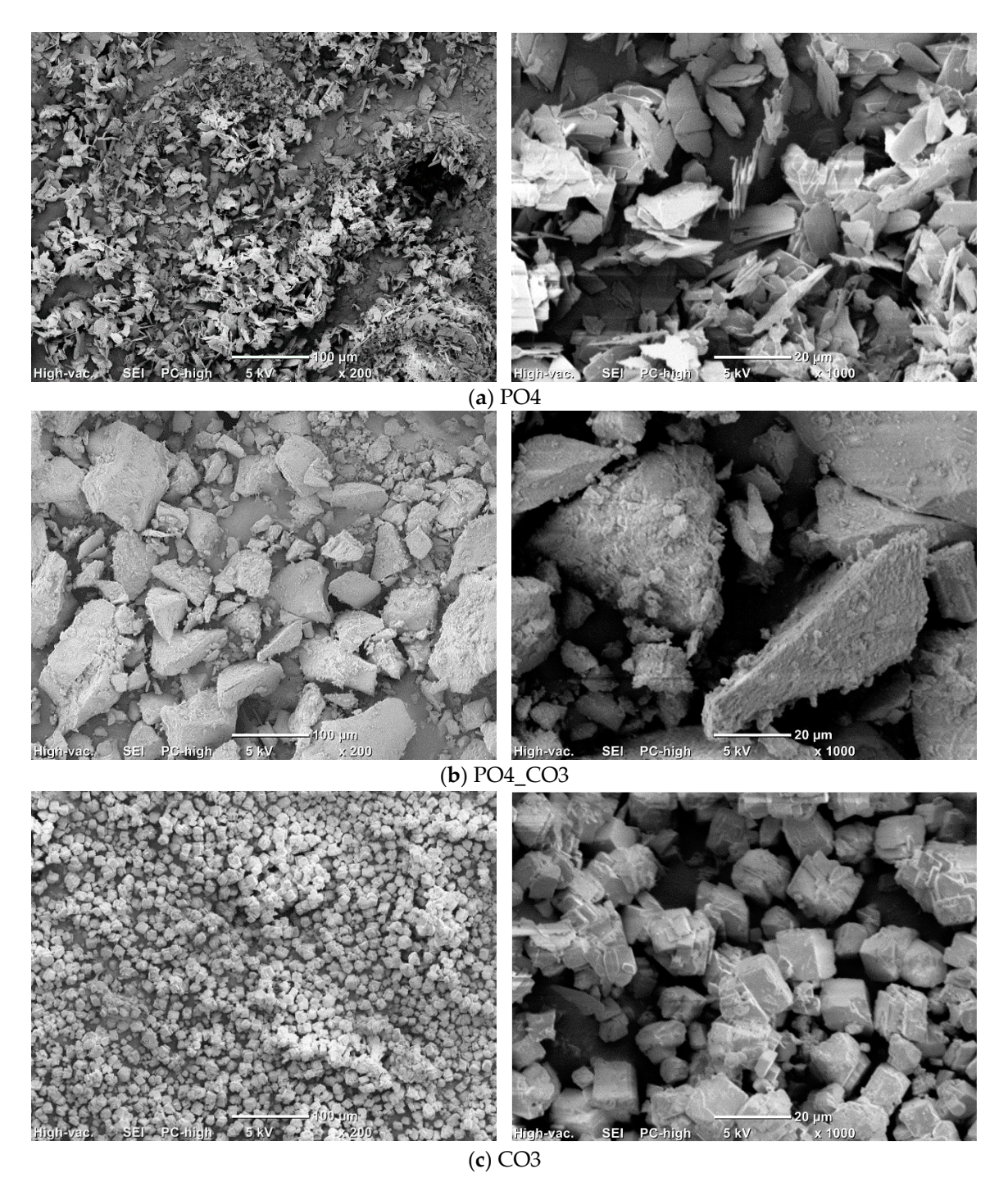


Figure 4. Micrographs of synthesized PO4 (a), PO4_CO3 (b), and CO3 (c) powders.

The particles of PO4 powder (Figure 4a) with a size of 10–20 microns and a thickness of 1–2 mm have a lamellar morphology characteristic of brushite (CaHPO $_4\cdot 2H_2O$) [64]. The particles of CO3 powder (Figure 4c) with a size of 10–20 mm have the cubic shapes, which is typical for calcite (CaCO $_3$) [65]. The PO4_CO3 powder (Figure 4b) is composed of large aggregates of 5–60 mm in size, consisting of particles less than 1 mm in size. Hydroxyapatite powders synthesized by precipitation from solutions, as a rule, consist of particles having a size of less than a micron [66]. It was estimated that the mass (33.5 g) of the synthesized PO4_CO3 powder after drying was 8.4 g higher than the expected (25.1 g) mass of the powder (Table 4). The mass of reaction by-product (PO4_CO3_by) isolated from the mother liquor was 11.8 g less than the expected (37.3 g) mass. Thus, after drying and grinding in a

Compounds 2025, 5, 41 10 of 23

mortar, KCl (reaction by-product) retained in the synthesized powder acted as a binder, binding hydroxyapatite particles in large aggregates visible in the micrographs (Figure 4b).

Phase composition of all synthesized powders included biocompatible phases of hydroxyapatite (PO4_CO3 powder), brushite (PO4 powder), and calcite (CO3 powder). For starting, all these powders can be recommended for the creation of composite materials with a polymer [35,67–69] or inorganic matrix [70]. Powders with a phase composition including brushite and hydroxyapatite, after removing reaction by-products, can be used for the preparation of ceramics with a phase composition in the CaO-P₂O₅ presented by β -Ca₂P₂O₇ [71,72] or β -Ca₃(PO₄)₂ [73–75], and in the CaO-P₂O₅-H₂O [76,77] oxide systems. Powder with a phase composition presented by calcite can be used for the preparation of biocompatible materials in the form of powder, granulate, or ceramics with phase composition in different oxide systems (for example, as mentioned above) as a precursor of CaO [42,78].

Figure 5 shows the TA data of the synthesized powders. According to the TGA data (Figure 5a), the total weight loss at 1000 °C for PO4 powder was 27.9%. The change in the weight of the PO4 powder is possible due to the removal of physically bound water, dehydration of brushite (CaHPO $_4$ ·2H $_2$ O), and the formation of monetite (CaHPO $_4$) (reaction 8), and the conversion of monetite (CaHPO $_4$) into pyrophosphate (Ca $_2$ P $_2$ O $_7$) (reaction 9).

$$CaHPO_4 \cdot 2H_2O \rightarrow CaHPO_4 + 2H_2O \tag{8}$$

$$2CaHPO_4 \rightarrow Ca_2P_2O_7 + H_2O \tag{9}$$

The theoretically possible mass loss during reactions 8 and 9 is 26.16%, which is close to the value of the total mass loss for PO4 powder determined by the TGA method. All the processes indicated for the PO4 powder, leading to weight loss, occur with heat absorption in the ranges 87–168 °C, 168–243 °C, and 375–477 °C (Figure 5b). It can be assumed that the presence of KCl in the PO4 powder, as well as the stage of thermostating the sample at 40 °C for 30 min before heating at a set rate (10 °C/min), causes decomposition of the metastable brushite at lower temperatures in the range of 87–168 °C (reaction 8). In [79], the authors conclude that two-stage conversion of brushite into monetite was possible with the formation of an amorphous phase at the first stage. The range 168–243 °C should be considered as characteristic of the monetite (CaHPO₄) formation from brushite (CaHPO₄·2H₂O) [80], and the range 375–477 °C should be considered as characteristic of the calcium pyrophosphate (Ca₂P₂O₇) from monetite (CaHPO₄) formation [81,82]. In the range of 477–840 °C, the smooth change in mass was 3%, while it is difficult to identify the intervals for processes that occur with heat absorption or release.

According to the TGA data (Figure 5a), the total weight loss at $1000\,^{\circ}\text{C}$ for the CO3 powder was 44.9%. The theoretically possible mass change for calcite during thermal decomposition in accordance with reaction (10) is 44%. The change in the mass of the CO3 powder occurred with heat absorption in the range 622–844 °C, amounted to 42.9% due to the decomposition of calcite and was accompanied by the release of CO₂ (reaction 10).

$$CaCO_3 \rightarrow CaO + CO_2$$
 (10)

The graph of the mass change of the CO3 powder (Figure 5a) and the dependence of the ion current on temperature (Figure 5c) have the forms characteristic of calcite CaCO₃ [83]. In Figure 5c, for the CO3 powder, one can see a graph of the dependence of the ion current on temperature for m/z = 44 (CO₂), typical for CaCO₃. It should be noted that in the range 844–949 °C, a loss (2%) of mass is observed, which is most likely associated with both the removal of CO₂ and the removal of that insignificant amount of KCl (Table 4), which could

Compounds 2025, 5, 41 11 of 23

be captured by the synthesized CO3 powder, above the melting point of KCl (776 $^{\circ}$ C [84] or 769 \pm 2 $^{\circ}$ C (1042 \pm 2 K) [85]).

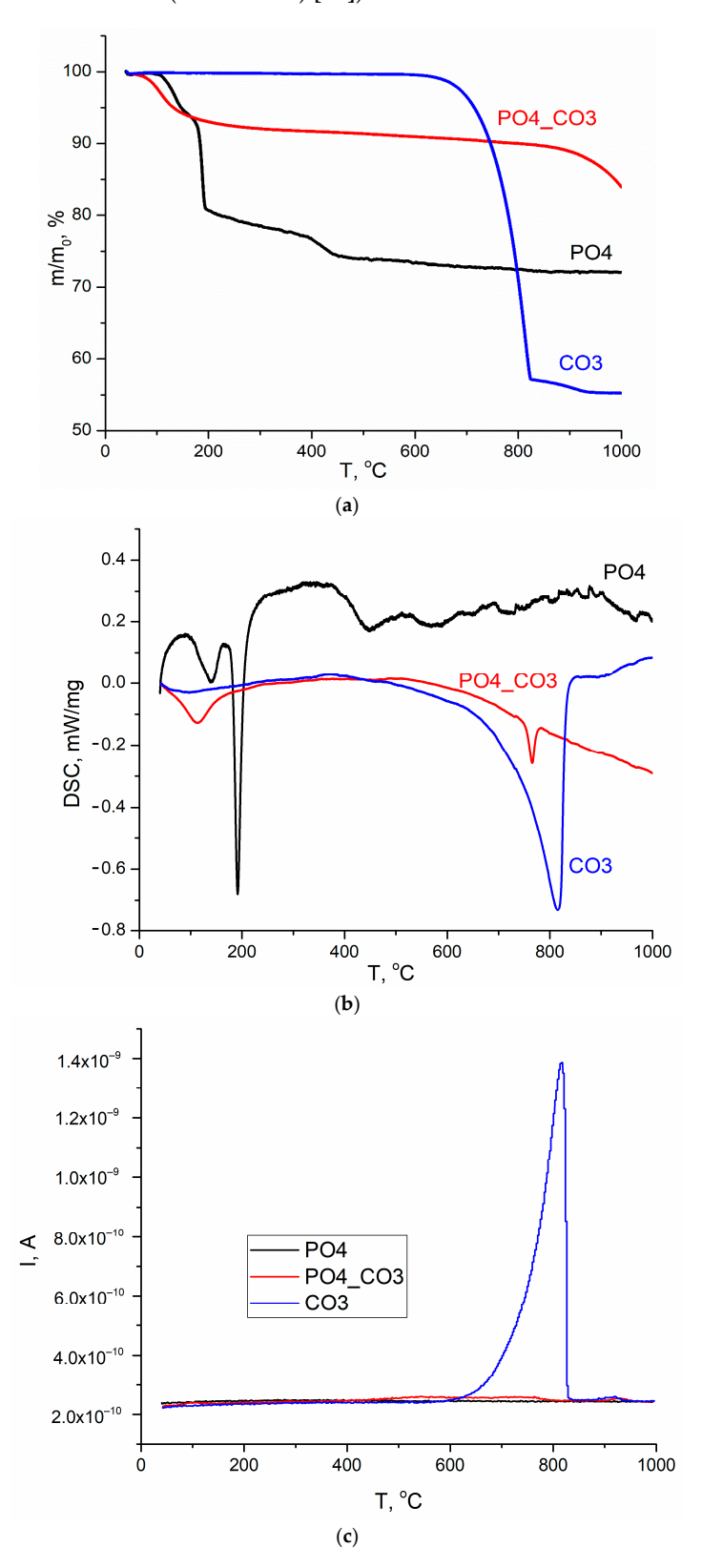


Figure 5. TA data of synthesized powders: TGA (a), DSC (b), MS for m/z = 44 (CO₂) (c).

According to the TGA data (Figure 5a), the total weight loss at $1000\,^{\circ}\text{C}$ for PO4_CO3 powder was 16.2%. Three sections can be distinguished on the curve of mass versus temperature for PO4_CO3 powder: removal of physically bound water (7.5% mass loss),

Compounds 2025, 5, 41 12 of 23

which proceeds with heat absorption in the range of 43–240 °C; a section of smooth weight reduction (2.6%) in the range of 240–829 °C; and a section of mass loss (6.1%), apparently related to the removal of KCl, in the range of 829–1000 °C. The endothermic peak at 765 °C, clearly seen on the DSC curve (Figure 5b), can be attributed to the melting of KCl, since according to the estimation (Table 4), the mass of the retained reaction by-product (KCl) in the PO4_CO3 powder was the maximum. No endothermic peaks that could be attributed to the KCl melting process were found in the DSC graphs for PO4 and CO3 powders synthesized for comparison. Significantly lower values of the ion current can be seen on the curve m/z = 44 (CO2) for PO4-CO3 powder (Figure 5c) in wide ranges of 460–800 °C and 900–940 °C than for CO3 powder.

Figure 6 shows the XRD of the CO3 powder synthesized from aqueous solutions of $CaCl_2$ and K_2CO_3 after heat treatment at various temperatures.

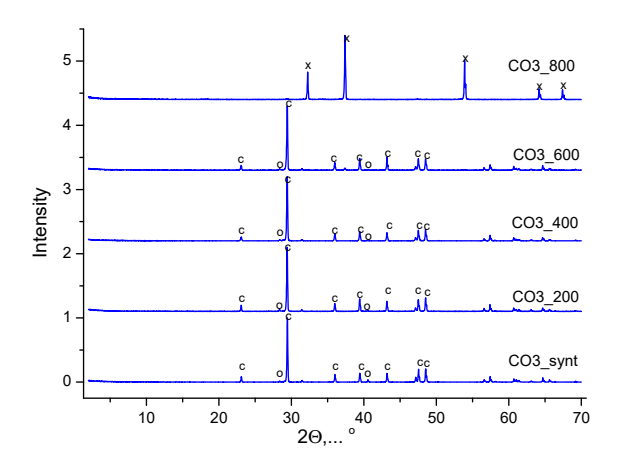


Figure 6. XRD data of CO3 powder after synthesis and after heat treatment at different temperatures. c—calcium carbonate (calcite, CaCO₃) (PDF card No 5-586; No 96-210-0190); o—potassium chloride (sylvine, KCl) (PDF No 41-1476; No 96-900-8652); x—calcium oxide (CaO) (PDF No 37-1497, No 96-101-1096).

According to the XRD data, the phase composition of the CO3 powder synthesized from aqueous solutions of $CaCl_2$ and K_2CO_3 , after heat treatment at various temperatures in the range of 200–600 °C for 2 h, was represented by calcite (CaCO₃). And after heat treatment at 800 °C, the phase composition of the CO3 powder was represented by calcium oxide (CaO) (reaction 10).

Figure 7 shows micrographs of CO3 powders after heat treatment for 2 h at various temperatures in the range of 200–600 °C. The particle size and shape of the powder particles after heat treatment did not significantly differ from the particle size and shape of the synthesized powder. It is difficult to detect particles with dimensions less than 2 mm and more than 20 mm in the micrographs.

Figure 8 shows the XRD of PO4 powder synthesized from aqueous solutions of CaCl₂ and K_2HPO_4 after heat treatment at various temperatures. After heat treatment at 200 °C for 2 h, the phase composition of the PO4_200 powder was represented by monetite CaHPO₄ (reaction 9). The phase composition of the PO4_400 and PO4_600 powders was represented by γ-calcium pyrophosphate (γ-Ca₂P₂O₇) (reaction 10) after heat treatment at 400 °C and at 600 °C for 2 h. The phase composition of the PO4_800 and PO4_1000 powders included β-tricalcium phosphate (β-Ca₃(PO₄)₂), β-calcium pyrophosphate (β-Ca₂P₂O₇), and calcium potassium pyrophosphate ($K_2CaP_2O_7$) after heat treatment at 800 °C and at 1000 °C for 2 h. According to data from Match! Software, after heat treatment at 1000 °C, PO4_1000 powder consisted of 43.7% of β-Ca₃(PO₄)₂, 41.7% of β-Ca₂P₂O₇, and 14.6% of $K_2CaP_2O_7$.

Compounds 2025, 5, 41 13 of 23

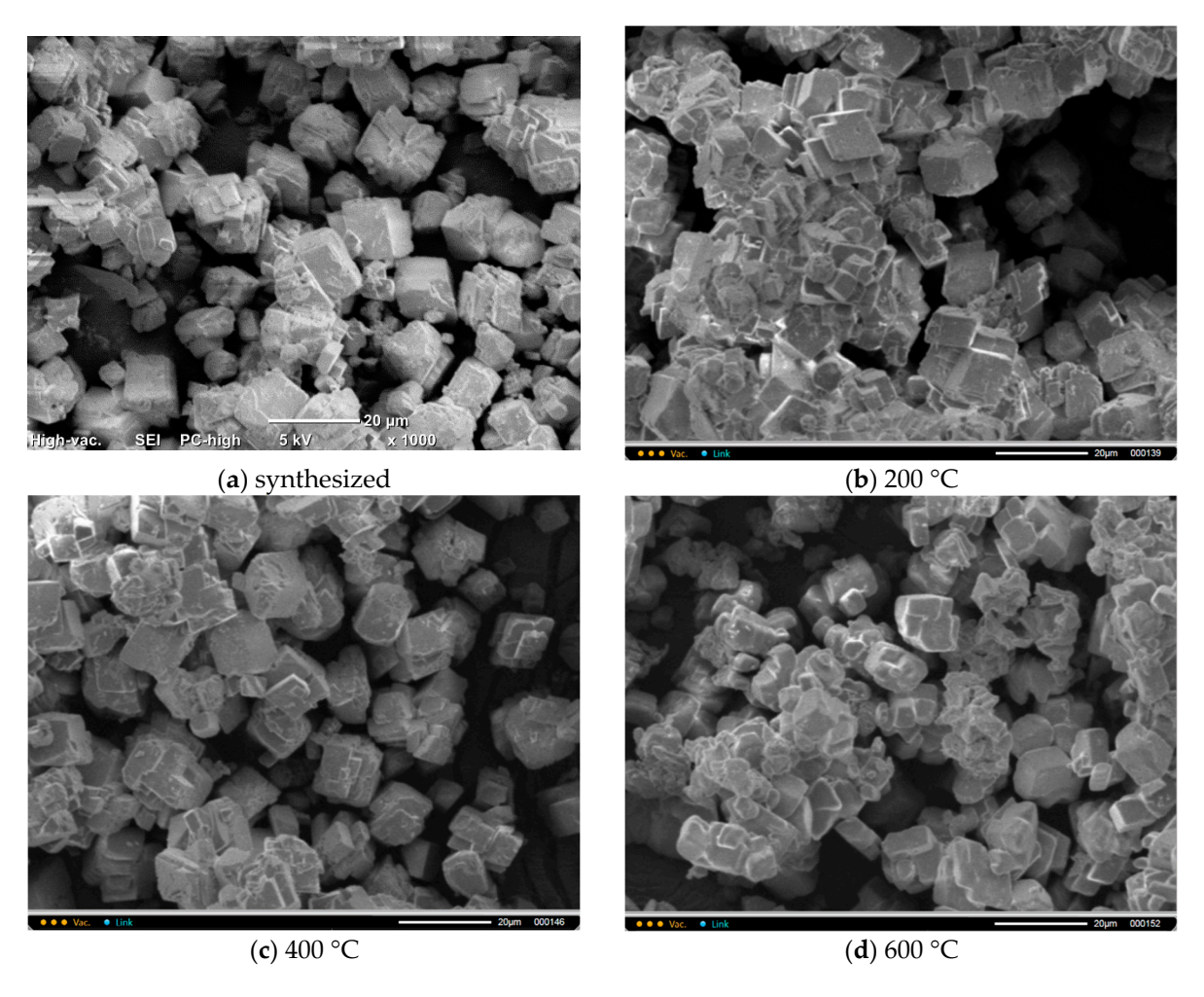


Figure 7. Microphotographs of CO3 powder after synthesis (**a**) and after heat treatment at different temperatures: $200 \,^{\circ}\text{C}$ (**b**), $400 \,^{\circ}\text{C}$ (**c**), $600 \,^{\circ}\text{C}$ (**d**).

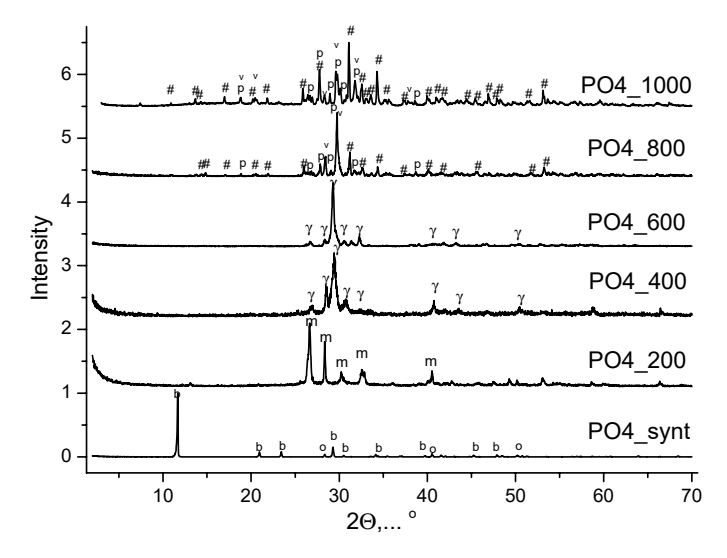


Figure 8. XRD data of PO4 powder after synthesis and after heat treatment at different temperatures. o—potassium chloride (sylvine, KCl) (PDF No 41-1476; No 96-900-8652); b—brushite (CaHPO₄·2H₂O) (PDF card No 9-77; No 96-231-0527); m—monetite (CaHPO₄) (PDF card No 9-80; 96-210-6185); γ — γ -calcium pyrophosphate (γ -Ca₂P₂O₇) (PDF card No 17-499); p— β -calcium pyrophosphate (β -Ca₂P₂O₇) (PDF card 9-346; No 96-100-1557); #— β -tricalcium phosphate (β -Ca₃(PO₄)₂) (PDF card No 9-169; No 96-151-7239); v—K₂CaP₂O₇ (PDF card No 22-805; No 96-220-2941).

Compounds 2025, 5, 41 14 of 23

Reaction (11) may reflect the formation of β -calcium orthophosphate (β -Ca₃(PO₄)₂) and calcium potassium pyrophosphate (K_2 CaP₂O₇):

$$2Ca_2P_2O_7 + 2KCl + H_2O \rightarrow Ca_3(PO_4)_2 + K_2CaP_2O_7 + 2HCl$$
 (11)

Figure 9 shows micrographs of PO4 powders after thermal treatment for 2 h at various temperatures in the range of 200–1000 $^{\circ}$ C. The particle size and shape of the powder particles after heat treatment at 200 and 400 $^{\circ}$ C practically do not differ from the particle size and shape of the synthesized powder. After heat treatment in the range of 600–1000 $^{\circ}$ C, as the temperature increases, the powder particles lose their lamellar morphology more and more. And after heat treatment at 1000 $^{\circ}$ C, the PO4_1000 powder is composed of conglomerates 5–20 microns in size, consisting of particles 1–3 microns in size, sintered together.

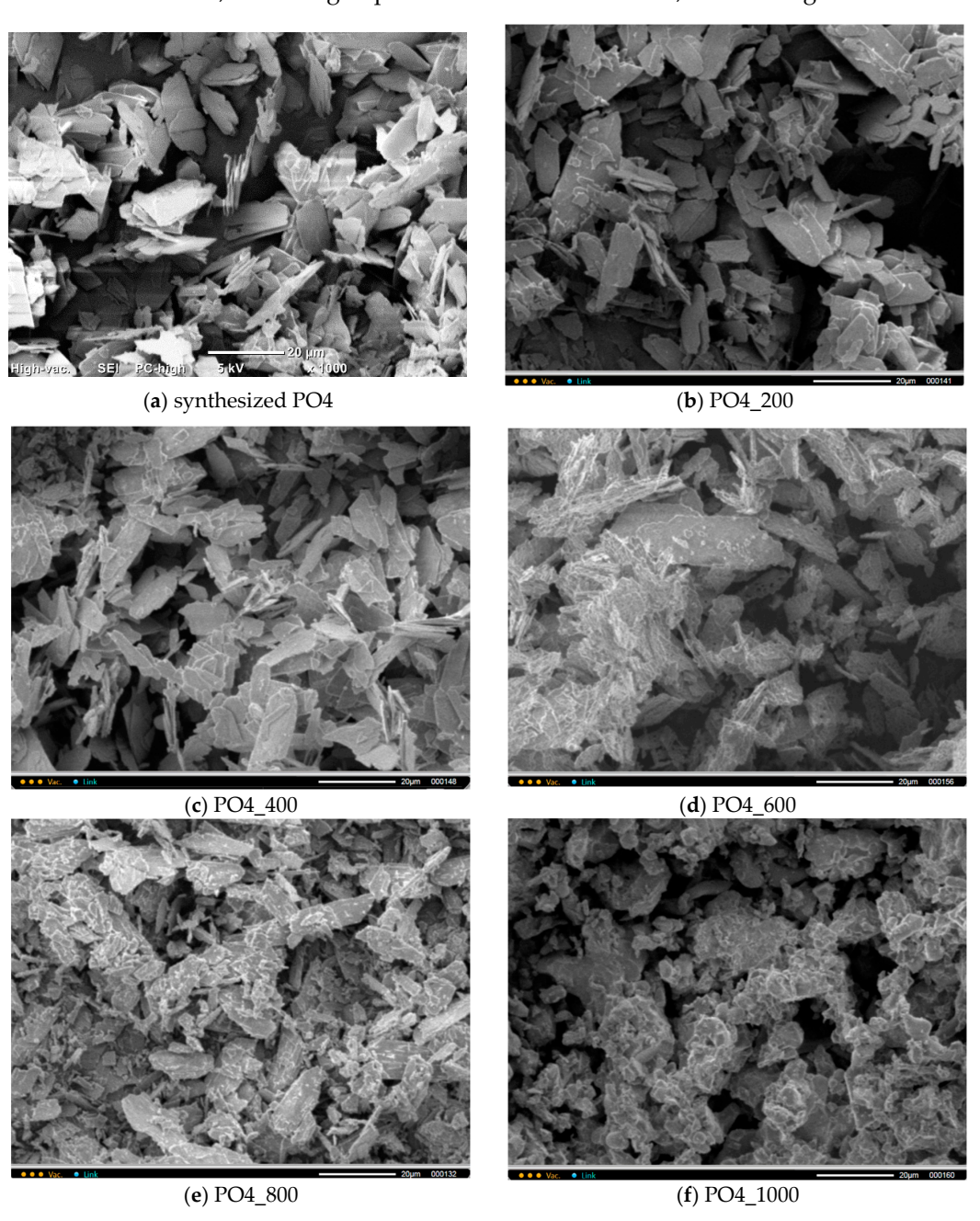


Figure 9. Micrographs of PO4 powder after synthesis (a) and after heat treatment at various temperatures: 200 (b), 400 (c), 600 (d), 800 (e), 1000 (f).

Compounds 2025, 5, 41 15 of 23

Figure 10 shows the FTIR data for PO4 and PO4_1000 powders, along with the XRD and SEM data, confirming the transformation of the synthesized powder after heat treatment at 1000 °C. After heat treatment of the PO4 powder at 1000 °C, according to the FTIR data, the presence of PO_4^{3-} groups remains and a $\delta(POP)$ 720 cm⁻¹ vibration appears, which confirms the presence of the pyrophosphate ion $P_2O_7^{4-}$ in both calcium pyrophosphate formed from brushite (reactions 8 and 9) and calcium potassium pyrophosphate (reaction 11).

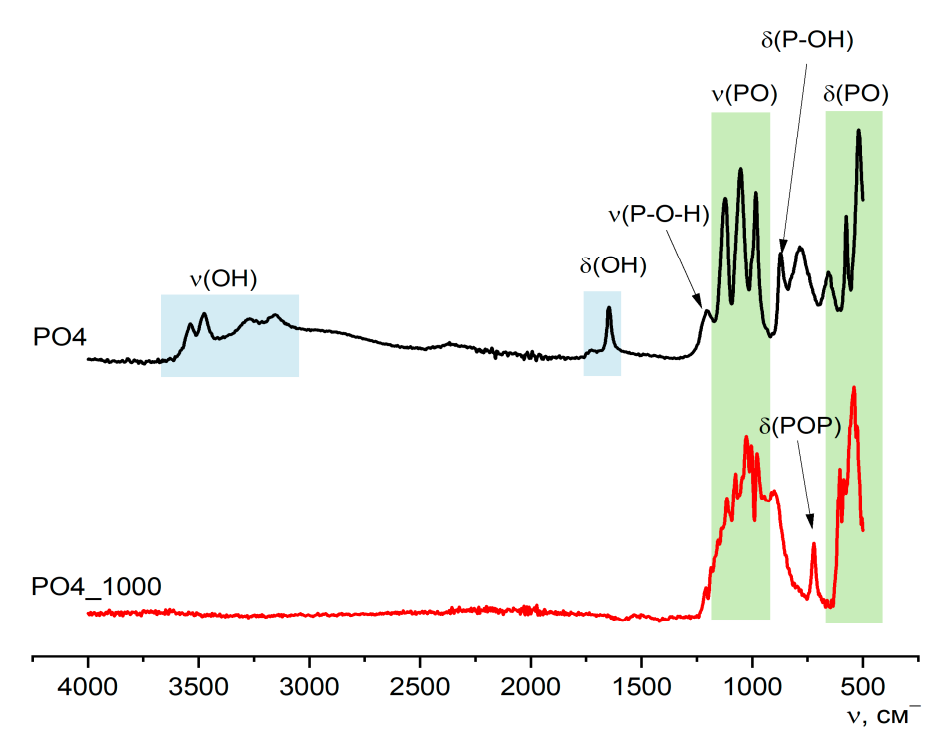


Figure 10. FTIR spectra of synthesized PO4 powder and PO4_1000 powder after heat treatment at 1000 °C.

Figure 11 shows the XRD of the PO4_CO3 powder synthesized from aqueous solutions of CaCl₂, KHPO₄, and K₂CO₃ after heat treatment at various temperatures. The phase composition of PO4_CO3 powders after thermal treatment in the range of 200–800 °C is represented by weakly crystallized hydroxyapatite and potassium chloride (sylvine, KCl). After heat treatment at 1000 °C, the phase composition of the PO4_CO3_1000 powder is represented by chlorapatite (Ca₁₀(PO₄)₆Cl₂). The formation of chlorapatite can be reflected by the reaction (12):

$$Ca_{10}(PO_4)_6(OH)_2 + 2KCl \rightarrow Ca_{10}(PO_4)_6Cl_2 + 2KOH$$
 (12)

A similar formation of chlorapatite was observed at 1000 $^{\circ}$ C from weakly crystalline hydroxyapatite of natural origin and sodium chloride (NaCl) [86], or in powder consisting of CaHPO₄·2H₂O, CaHPO₄, and NaCl when heated at a range of 800–1100 $^{\circ}$ C [17].

Micrographs of PO4_CO3 powder after synthesis and after heat treatment at various temperatures are presented in Figure 12. The microstructure of PO4_CO3 powders, after thermal treatment in the range of 200–800 $^{\circ}$ C, does not significantly differ from the microstructure of the powder after synthesis and drying. Powders consist of sufficiently large agglomerates (up to 100–200 mm) consisting of particles of weakly crystallized hydroxyapatite bonded with reaction by-product KCl. The microstructure of the PO4_CO3_1000 powder after heat treatment at 1000 $^{\circ}$ C differs significantly from the microstructure of powders after heat treatment in the range of 200–800 $^{\circ}$ C. The PO4_CO3_1000 powder after

Compounds 2025, 5, 41 16 of 23

heat treatment at 1000 °C consists of particles with a prismatic shape 5–20 mm long and a transverse dimension of 2–5 mm. In the micrograph (Figure 12e, left side) with a lower magnification, one can see loose aggregates up to 100 microns in size, consisting of the prismatic particles mentioned above.

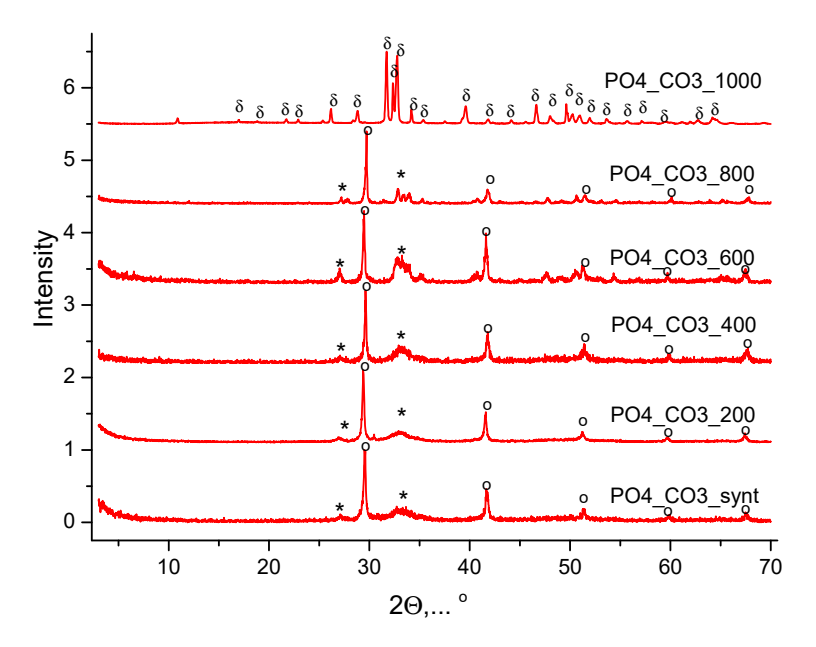


Figure 11. XRD data of PO4_CO3 powder after synthesis and after heat treatment at different temperatures. *—hydroxyapatite ($Ca_{10}(PO_4)_6(OH)_2$) (PDF No 96-901-4314); o—potassium chloride (sylvine, KCl) (PDF No 41-1476; No 96-900-8652); δ —chlorapatite ($Ca_{10}(PO_4)_6Cl_2$) (PDF No 73-1728; No 96-101-0917).

Figure 13 shows the FTIR spectroscopy data for PO4_CO3 powder after synthesis and after heat treatment at 1000 °C. In the spectrum of the PO4_CO3_1000 powder, there are no peaks that could be attributed to ν (OH), ν (CO3²⁻), or π (CO3²⁻). The FTIR spectrum for the PO4_CO3_1000 powder corresponds to the reference data for chlorapatite (Spectra-Base Compound ID KKRjtSFM3Pp, https://spectrabase.com/spectrum/KKRjtSFM3Pp (accessed on 23 August 2025)).

Powder with the phase composition in the K₂O-CaO-P₂O₅ system, including β -calcium pyrophosphate (β -Ca₂P₂O₇), β -calcium orthophosphate (β -Ca₃(PO₄)₂), and potassium calcium pyrophosphate (K₂CaP₂O₇) can be prepared from synthesized powder PO4 consisting of brushite and KCl. Phase composition after heat treatment at temperatures 800 and 1000 °C for PO4 powder included such biocompatible phases as β-calcium pyrophosphate (β-Ca₂P₂O₇) [62] and β-calcium orthophosphate (β-Ca₃(PO₄)₂) [87]. Minerals in the K₂O-CaO-P₂O₅ system are under consideration as biocompatible [88,89]. Nevertheless, potassium calcium pyrophosphate (K₂CaP₂O₇), according to the scientific literature, is known as a matrix for luminescent materials [90], or it was mentioned as the most promising fertilizer material [91]. Taking into account the possibility for K₂CaP₂O₇ to be used as fertilizer material and the relatively low (14.6%) content of K₂CaP₂O₇ in the PO4_1000 powder, it is possible to expect that materials that can be created based on PO4_1000 powder will be treated as biocompatible after ordinary tests in vitro and in vivo. Powder of chlorapatite (Ca₁₀(PO₄)₆Cl₂) can be prepared from synthesized PO₄_CO₃ powder consisting of hydroxyapatite ($Ca_{10}(PO_4)_6(OH)_2$) and KCl at 1000 °C. Chlorapatite ($Ca_{10}(PO_4)_6Cl_2$) can also be used both as a matrix for the creation of luminescent materials [92] and as a component of biocompatible materials [93].

Compounds **2025**, 5, 41 17 of 23

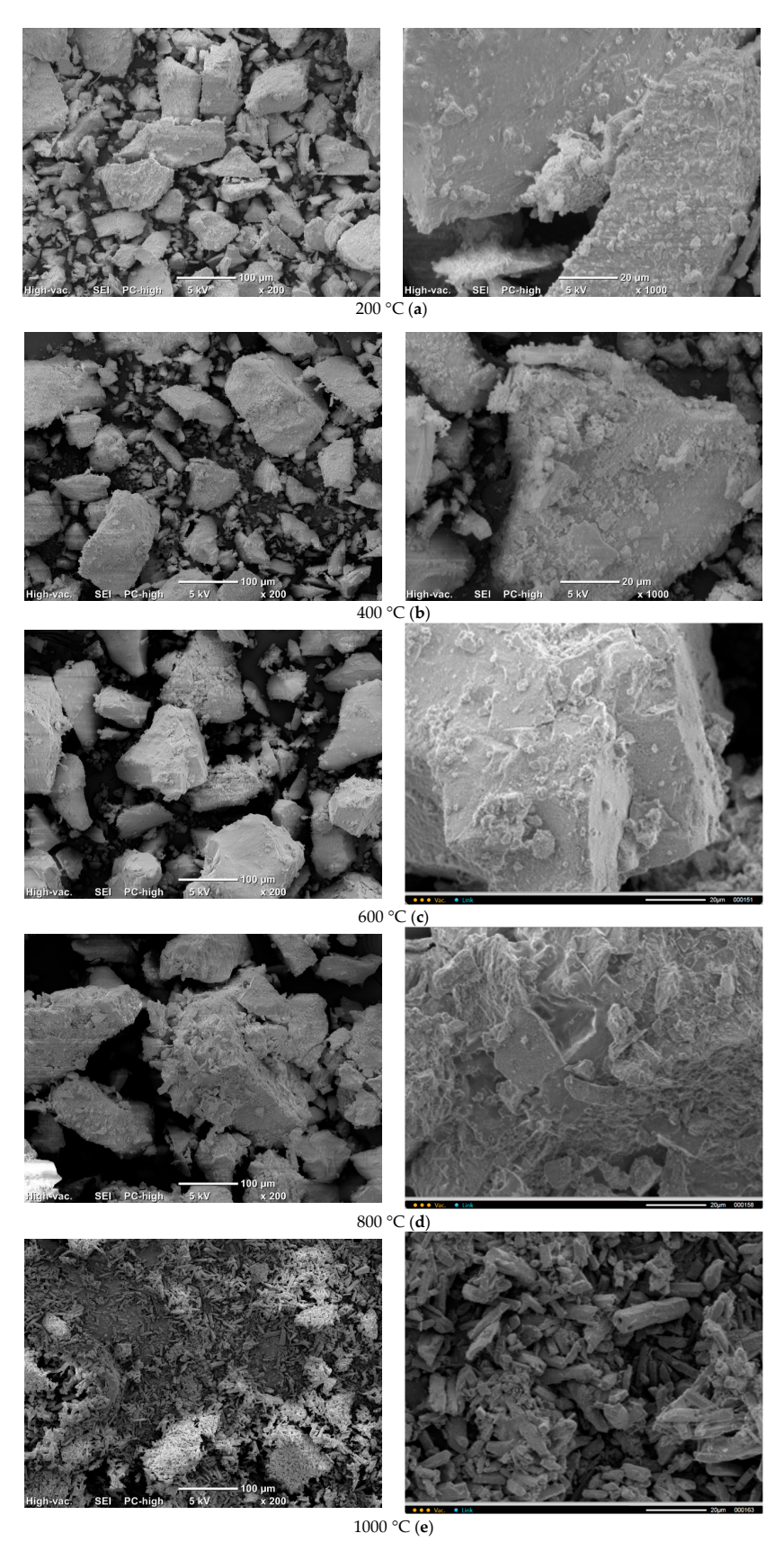


Figure 12. Micrographs of PO4_CO3 powder after heat treatment at various temperatures: 200 (a), 400 (b), 600 (c), 800 (d), 1000 (e).

Compounds 2025, 5, 41 18 of 23

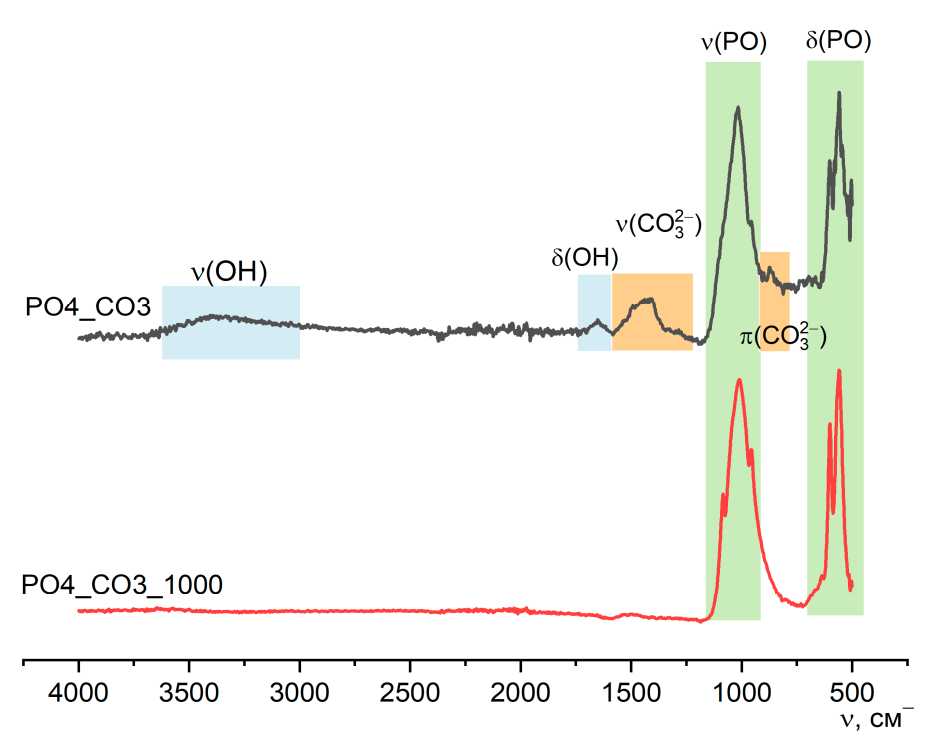


Figure 13. FTIR spectra of PO4_CO3 powder after synthesis and after heat treatment at 1000 °C.

4. Conclusions

Powders with the phase composition including target products such as brushite (CaHPO $_4$ ·2H $_2$ O), and calcium carbonate (calcite, CaCO $_3$), as well as potassium chloride (sylvine, KCl), as a reaction by-product, were synthesized from aqueous solutions of calcium chloride (CaCl $_2$), potassium hydrophosphate (K $_2$ HPO $_4$), and potassium carbonate (K $_2$ CO $_3$). The interaction of an aqueous mixed-anionic solution including HPO $_4$ ²⁻ and CO $_3$ ²⁻ anions and an aqueous solution of calcium chloride (CaCl $_2$), made it possible to obtain a powder that combined weakly crystallized hydroxyapatite and a significant amount (estimated to be up to 30–35% by weight) of potassium chloride (sylvine, KCl), in its phase composition. The XRD, SEM, and FTIR data confirmed the possibility of synthesizing chlorapatite (Ca $_{10}$ (PO $_4$) $_6$ Cl $_2$) from this powder via heat treatment at 1000 °C for 2 h.

After heat treatment of the synthesized powder containing brushite (CaHPO $_4$ ·2H $_2$ O), and potassium chloride (sylvine, KCl), at 800 and 1000 °C, powders with the phase composition including β -calcium pyrophosphate (β -Ca $_2$ P $_2$ O $_7$), β -calcium orthophosphate (β -Ca $_3$ (PO $_4$) $_2$), and potassium calcium pyrophosphate (K $_2$ CaP $_2$ O $_7$) were obtained. Heat treatment of calcite (CaCO $_3$) powder at 800 °C, as was expected, led to the formation of calcium oxide (CaO).

Powders including phases such as hydroxyapatite, chlorapatite, brushite, monetite, calcium pyrophosphate, calcium potassium pyrophosphate, tricalcium phosphate, and calcite can be used for the creation of biocompatible inorganic materials or composite materials with a biocompatible polymer matrix. Powders of chlorapatite can be used as a matrix for the creation of luminescent materials. Potassium chloride (sylvine, KCl), present in synthesized powders can act as one of the precursors of chlorapatite or calcium potassium pyrophosphate, or it can act as a removable inorganic porogen.

Compounds 2025, 5, 41 19 of 23

Author Contributions: Conceptualization, T.V.S.; methodology, T.V.S.; investigation, T.V.S., H.M.N.L., T.B.S., A.M.M., T.V.F., E.A.M., D.M.T., D.O.G., O.V.B. and A.V.K.; resources, T.V.S., T.B.S., D.M.T. and O.V.B.; writing—original draft preparation, T.V.S. and H.M.N.L.; writing—review and editing, T.V.S.; visualization, T.V.S., H.M.N.L., T.B.S., A.M.M., T.V.F., D.M.T., D.O.G., O.V.B. and A.V.K.; supervision, T.V.S.; project administration, T.V.S.; funding acquisition, T.V.S. All authors have read and agreed to the published version of the manuscript.

Funding: This work was carried out with the support of the State assignment of the Lomonosov Moscow State University: AAAA-A21-121011590082-2.

Data Availability Statement: The original contributions presented in this study are included in the article. Further inquiries can be directed to the corresponding author.

Acknowledgments: This research was carried out using the equipment of the MSU Shared Research Equipment Center "Technologies for obtaining new nanostructured materials and their complex study" and was purchased by MSU within the framework of the Equipment Renovation Program (National Project "Science") and within the framework of the MSU Program of Development.

Conflicts of Interest: The authors declare no conflicts of interest.

References

- 1. Andrianov, N.T.; Balkevich, V.L.; Belyakov, A.V.; Vlasov, A.S.; Guzman, I.Y.; Lukin, E.S.; Mosin, Y.M.; Skidan, B.S. Chemical technology of ceramics: Textbook. In *Handbook for Universities*; Guzmanm, I.Y., Ed.; Rif Stroymaterialy LLC: Moscow, Russia, 2012; 496p, ISBN 978-5-94026-01966. (In Russian)
- 2. Butt, Y.M.; Sychev, M.M.; Timashev, V.V. Chemical technology of binder materials. In *Textbook for Universities on Spec. "Chemical Technology of Binding Materials"*; Timashev, V.V., Ed.; Higher School: Moscow, Russia, 1980; 472p. ill., 22. (In Russian)
- 3. Lee, B.; Komarneni, S. (Eds.) *Chemical Processing of Ceramics*; CRC Press: Boca Raton, FL, USA, 2005; 756p, ISBN 978-0-42911-963-7. [CrossRef]
- 4. Gerasimov, M.D.; Latyshev, S.S.; Bogdanov, N.E.; Loktionov, I.O. Review of constructive solutions in the field of grinding mills. In *Energy-Saving Technological Complexes and Equipment for the Production of Building Materials: An Interuniversity Collection of Articles*; Bogdanov, V.S., Ed.; Volume Issue XVII; Belgorod State Technological University named after V.G. Shukhov: Belgorod, Russia, 2018; pp. 132–146. Available online: https://www.elibrary.ru/item.asp?id=42997967 (accessed on 23 August 2025). (In Russian)
- 5. Shlyakhtin, O.A.; Tretyakov, Y.D. Recent progress in cryochemical synthesis of oxide materials. *J. Mater. Chem.* **1999**, *9*, 19–24. [CrossRef]
- Kageyama, H.; Ogino, H. (Eds.) Mixed-Anion Compounds; Special Collection: 2024 eBook Collection; Royal Society of Chemistry RSC: Cambridge, UK, 024; 276p, ISBN 978-1-83916-512-2. [CrossRef]
- 7. Lukin, E.S.; Makarov, N.A.; Kozlov, A.I.; Popova, N.A.; Anufrieva, E.V.; Vartanyan, M.A.; Kozlov, I.A.; Safina, M.N.; Lemeshev, D.O.; Gorelik, E.I. Oxide ceramics of the new generation and areas of application. *Glass Ceram.* **2008**, *65*, 348–352. [CrossRef]
- 8. Lukin, E.S. Modern high-density oxide ceramics with controlled microstructure. Part I. Effect of aggregation of oxide powders on the sintering and microstructure of ceramics. *Refractories* **1996**, 37, 6–14. [CrossRef]
- 9. Ring, T.A. Fundamentals of Ceramic Powder Processing and Synthesis, 1st ed.; Elsevier: Amsterdam, The Netherlands; Academic Press, Elsevier: Cambridge, MA, USA, 30 April 1996; ISBN 9780080532196. [CrossRef]
- 10. Safronova, T.V.; Putlyaev, V.I.; Filippov, Y.Y.; Shatalova, T.B.; Fatin, D.S. Ceramics Based on Brushite Powder Synthesized from Calcium Nitrate and Disodium and Dipotassium Hydrogen Phosphates. *Inorg. Mater.* **2018**, *54*, 195–207. [CrossRef]
- 11. Safronova, T.V.; Knot'ko, A.V.; Shatalova, T.B.; Evdokimov, P.V.; Putlyaev, V.I.; Kostin, M.S. Calcium phosphate ceramic based on powder synthesized from a mixed-anionic solution. *Glass Ceram.* **2016**, *73*, 25–31. [CrossRef]
- 12. Safronova, T.V.; Putlyaev, V.I.; Filippov, Y.Y.; Knot'ko, A.V.; Klimashina, E.S.; Peranidze, K.K.; Evdokimov, P.V.; Vladimirova, S.A. Powders synthesized from calcium acetate and mixed-anionic solutions, containing orthophosphate and carbonate ions, for obtaining bioceramic. *Glass Ceram.* **2018**, *75*, 118–123. [CrossRef]
- 13. Song, Y.; Hahn, H.H.; Hoffmann, E. The effect of carbonate on the precipitation of calcium phosphate. *Environ. Technol.* **2002**, 23, 207–215. [CrossRef]
- 14. Frank-Kamenetskaya, O.; Kol'tsov, A.; Kuz'mina, M.; Zorina, M.; Poritskaya, L. Ion substitutions and non-stoichiometry of carbonated apatite-(CaOH) synthesised by precipitation and hydrothermal methods. *J. Mol. Struct.* **2011**, 992, 9–18. [CrossRef]
- 15. Peranidze, K.; Safronova, T.V.; Filippov, Y.; Kazakova, G.; Shatalova, T.; Rau, J.V. Powders Based on Ca₂P₂O₇-CaCO₃-H₂O System as Model Objects for the Development of Bioceramics. *Ceramics* **2022**, *5*, 423–434. [CrossRef]

Compounds 2025, 5, 41 20 of 23

16. Golubchikov, D.; Safronova, T.V.; Nemygina, E.; Shatalova, T.B.; Tikhomirova, I.N.; Roslyakov, I.V.; Khayrutdinova, D.; Platonov, V.; Boytsova, O.; Kaimonov, M.; et al. Powder Synthesized from Aqueous Solution of Calcium Nitrate and Mixed-Anionic Solution of Orthophosphate and Silicate Anions for Bioceramics Production. *Coatings* **2023**, *13*, 374. [CrossRef]

- 17. Safronova, T.V.; Khantimirov, A.S.; Shatalova, T.B.; Filippov, Y.Y.; Kolesnik, I.V.; Knotko, A.V. Powders Synthesized from Solutions of Calcium Chloride, Sodium Hydrogen Phosphate, and Sodium Sulfate for Bioceramics Production. *Ceramics* **2023**, *6*, 561–583. [CrossRef]
- 18. Rey, C.; Combes, C.; Drouet, C.; Glimcher, M.J. Bone mineral: Update on chemical composition and structure. *Osteoporos. Int.* **2009**, 20, 1013–1021. [CrossRef] [PubMed]
- 19. Abe, M.; Costantino, U.; Alberti, G.; Howe, A.T.; Ruvarac, A. *Inorganic Ion Exchange Materials*; Clearfield, A., Ed.; CRC Press: Boca Raton, FL, USA, 2018; 297p, ISBN 0-8493-5930-9.
- Ivanets, A.I.; Shashkova, I.L.; Kitikova, N.V.; Radkevich, A.V.; Davydov, Y.P. Recovery of strontium ions with calcium and magnesium phosphates from aqueous solutions against the background of CaCl₂. Radiochemistry 2015, 57, 610–615. [CrossRef]
- 21. Berlyand, A.S.; Snyakin, A.P.; Prokopov, A.A. Adsorption capacity of hydroxyapatite for several amino acids and heavy metal ions. *Pharm. Chem. J.* **2012**, *46*, 292. [CrossRef]
- 22. Bystrov, V.S.; Paramonova, E.V.; Filippov, S.V.; Likhachev, I.V.; Bystrova, A.V.; Avakyan, L.A.; Kovrigina, S.A.; Makarova, S.V.; Bulina, N.V. Features of the Structure and Properties of Hydroxypapatite with Various Cationic Substitutions. In *Proceedings of the International Conference "Mathematical Biology and Bioinformatics"*; Lakhno, V.D., Ed.; IMPB RAS: Pushchino, Russia, 2024; Volume 10, Paper No. e11. (In Russian) [CrossRef]
- 23. Tite, T.; Popa, A.-C.; Balescu, L.M.; Bogdan, I.M.; Pasuk, I.; Ferreira, J.M.F.; Stan, G.E. Cationic Substitutions in Hydroxyapatite: Current Status of the Derived Biofunctional Effects and Their In Vitro Interrogation Methods. *Materials* **2018**, *11*, 2081. [CrossRef]
- 24. Jiang, Y.; Yuan, Z.; Huang, J. Substituted hydroxyapatite: A recent development. Mater. Technol. 2020, 35, 785–796. [CrossRef]
- 25. DileepKumar, V.G.; Sridhar, M.S.; Aramwit, P.; Krut'ko, V.K.; Musskaya, O.N.; Glazov, I.E.; Reddy, N. A review on the synthesis and properties of hydroxyapatite for biomedical applications. *J. Biomater. Sci. Polym. Ed.* **2022**, *33*, 229–261. [CrossRef]
- Alam, M.K.; Hossain, M.S.; Kawsar, M.; Bahadur, N.M.; Ahmed, S. Synthesis of nano-hydroxyapatite using emulsion, pyrolysis, combustion, and sonochemical methods and biogenic sources: A review. RSC Adv. 2024, 14, 3548–3559. [CrossRef]
- 27. Sezanova, K.; Tuparova, Y.; Shestakova, P.; Markov, P.; Kovacheva, D.; Rabadjieva, D. Calcium Phosphate Ceramic Powders Prepared from Mechanochemically Activated Precursors. *Inorganics* **2025**, *13*, 313. [CrossRef]
- 28. Balbuena, O.B.F.; Paiva, L.F.S.; Ribeiro, A.A.; Monteiro, M.M.; de Oliveira, M.V.; Pereira, L.C. Sintering parameters study of a biphasic calcium phosphate bioceramic synthesized by alcoholic sol-gel technique. *Ceram. Int.* **2021**, *47*, 32979–32987. [CrossRef]
- 29. Jimoh, O.A.; Ariffin, K.S.; Hussin, H.B.; Temitope, A.E. Synthesis of precipitated calcium carbonate: A review. *Carbonates Evaporites* **2018**, 33, 331–346. [CrossRef]
- 30. Cai, J.; Lu, M.; Huang, Q.; Bai, F.; Zhao, D.; Jiang, H.; Chen, J. A Review of Nano-Calcium Carbonate and Its Applications: Preparation, Necessities, Biomedicine, and Environment. *Part. Part. Syst. Charact.* **2025**, e00093. [CrossRef]
- 31. Parushev, I.; Gerova-Vatsova, T. Methods for obtaining synthetic carbonate apatite for bone regeneration: A review. *Scr. Sci. Med. Dent.* **2025**, *11*, 7–17. Available online: https://journals.mu-varna.bg/index.php/ssmd/article/view/9879/8863 (accessed on 23 August 2025).
- 32. Kapolos, J.; Koutsoukos, P.G. Formation of calcium phosphates in aqueous solutions in the presence of carbonate ions. *Langmuir* **1999**, *15*, 6557–6562. [CrossRef]
- 33. Miron, R.J.; Fujioka-Kobayashi, M.; Pikos, M.A.; Nakamura, T.; Imafuji, T.; Zhang, Y.; Shinohara, Y.; Sculean, A.; Shirakata, Y. The development of non-resorbable bone allografts: Biological background and clinical perspectives. *Periodontol.* 2000 **2024**, 94, 161–179. [CrossRef]
- 34. He, F.; Zhang, J.; Tian, X.; Wu, S.; Chen, X. A facile magnesium-containing calcium carbonate biomaterial as potential bone graft. *Colloid. Surf. B* **2015**, *136*, 845–852. [CrossRef]
- 35. Huang, Y.; Cao, L.; Parakhonskiy, B.V.; Skirtach, A.G. Hard, Soft, and Hard-and-Soft Drug Delivery Carriers Based on CaCO₃ and Alginate Biomaterials: Synthesis, Properties, Pharmaceutical Applications. *Pharmaceutics* **2022**, 14, 909. [CrossRef]
- 36. Liu, H.; Wen, Z.; Liu, Z.; Yang, Y.; Wang, H.; Xia, X.; Ye, J.; Liu, Y. Unlocking the potential of amorphous calcium carbonate: A star ascending in the realm of biomedical application. *Acta Pharm. Sin. B* **2024**, *14*, 602–622. [CrossRef]
- 37. Liu, D.; Cui, C.; Chen, W.; Shi, J.; Li, B.; Chen, S. Biodegradable Cements for Bone Regeneration. *J. Funct. Biomater.* **2023**, *14*, 134. [CrossRef]
- 38. Bohner, M. Bioresorbable ceramics. In *Degradation Rate of Bioresorbable Materials*; Buchanan, F., Ed.; Woodhead Publishing: Sawston, UK, 2008; pp. 95–114. ISBN 978-1-84569-329-9. [CrossRef]
- 39. Min, K.H.; Kim, D.H.; Kim, K.H.; Seo, J.-H.; Pack, S.P. Biomimetic Scaffolds of Calcium-Based Materials for Bone Regeneration. *Biomimetics* **2024**, *9*, 511. [CrossRef]
- 40. Mishchenko, O.; Yanovska, A.; Kosinov, O.; Maksymov, D.; Moskalenko, R.; Ramanavicius, A.; Pogorielo, M. Synthetic Calcium–Phosphate Materials for Bone Grafting. *Polymers* 2023, 15, 3822. [CrossRef] [PubMed]

Compounds **2025**, 5, 41 21 of 23

41. Tavoni, M.; Dapporto, M.; Tampieri, A.; Sprio, S. Bioactive Calcium Phosphate-Based Composites for Bone Regeneration. *J. Compos. Sci.* **2021**, *5*, 227. [CrossRef]

- 42. Lunetta, E.; Messina, M.; Cacciotti, I. Doped hydroxyapatite bioceramic from food wastes for orthopedic applications. *J. Am. Ceram. Soc.* **2025**, *108*, e70002. [CrossRef]
- 43. ICDD. *PDF-4*+ 2010 (*Database*); Kabekkodu, S., Ed.; International Centre for Diffraction Data: Newtown Square, PA, USA, 2010; Available online: http://www.icdd.com/pdf-2/ (accessed on 23 August 2025).
- 44. Nakamoto, K. *Infrared and Raman Spectra of Inorganic and Coordination Compounds*, 5th ed.; Wiley: New York, NY, USA, 1986; pp. 156–159.
- 45. Lakshmi, D.S.; K. S., R.; Castro-Muñoz, R.; Tańczyk, M. Emerging Trends in Porogens toward Material Fabrication: Recent Progresses and Challenges. *Polymers* **2022**, *14*, 5209. [CrossRef]
- 46. Safronova, T.V.; Shatalova, T.B.; Filippov, Y.Y.; Toshev, O.U.; Knot'ko, A.V.; Vaimugin, L.A.; Savchenkova, D.V. Na₂O–CaO–SO₃ Ceramics as Promising Inorganic Porogens. *Glass Ceram.* **2022**, *79*, 88–94. [CrossRef]
- 47. Şahin, E.; Çiftçioğlu, M. Compositional, microstructural and mechanical effects of NaCl porogens in brushite cement scaffolds. *J. Mech. Behav. Biomed. Mater.* **2021**, *116*, 104363. [CrossRef]
- 48. Golubko, N.V.; Kaleva, G.M.; Mosunov, A.V.; Politova, E.D.; Sadovskaya, N.V.; Stefanovich, S.Y.; Segalla, A.H. Effects of KCl/LiF additives on the structure, phase transitions and dielectric properties of BSPT ceramics. *Ferroelectrics* **2015**, *485*, 95–100. [CrossRef]
- 49. Nzihou, A.; Adhikari, B.; Pfeffer, R. Effect of metal chlorides on the sintering and densification of hydroxyapatite adsorbent. *Ind. Eng. Chem. Res.* **2005**, *44*, 1787–1794. [CrossRef]
- 50. Diaz, J.C.C.A.; Muccillo, E.N.d.S.; Muccillo, R. Porous 8YSZ Ceramics Prepared with Alkali Halide Sacrificial Additives. *Materials* **2023**, *16*, 3509. [CrossRef]
- 51. Golubchikov, D.O.; Safronova, T.V.; Podlyagin, V.A.; Shatalova, T.B.; Kolesnik, I.V.; Putlayev, V.I. Silicate-substituted hydroxyapatite bioceramics fabrication from the amorphous powder precursor obtained from the silicate-containing solutions. *Mendeleev Commun.* 2024, 34, 847–849. [CrossRef]
- 52. Safronova, T.V.; Sterlikov, G.S.; Kaimonov, M.R.; Shatalova, T.B.; Filippov, Y.Y.; Toshev, O.U.; Roslyakov, I.V.; Kozlov, D.A.; Tikhomirova, I.N.; Akhmedov, M.R. Composite Powders Synthesized from the Water Solutions of Sodium Silicate and Different Calcium Salts (Nitrate, Chloride, and Acetate). *J. Compos. Sci.* 2023, 7, 408. [CrossRef]
- 53. Casciani, F.; Condrate, R.A., Sr. The vibrational spectra of brushite, CaHPO₄·2H₂O. Spectrosc. Lett. 1979, 12, 699–713. [CrossRef]
- 54. Berry, E.E.; Baddiel, C.B. The infra-red spectrum of dicalcium phosphate dihydrate (brushite). *Spectrochim. Acta A-M.* **1967**, 23, 2089–2097. [CrossRef]
- 55. Hirsch, A.; Azuri, I.; Addadi, L.; Weiner, S.; Yang, K.; Curtarolo, S.; Kronik, L. Infrared absorption spectrum of brushite from first principles. *Chem. Mater.* **2014**, *26*, 2934–2942. [CrossRef]
- 56. Wang, X.; Xu, X.; Ye, Y.; Wang, C.; Liu, D.; Shi, X.; Wang, S.; Zhu, X. In-situ High-Temperature XRD and FTIR for Calcite, Dolomite and Magnesite: Anharmonic Contribution to the Thermodynamic Properties. *J. Earth Sci.* **2019**, *30*, 964–976. [CrossRef]
- 57. Bosch Reig, F.; Gimeno Adelantado, J.V.; Moya Moreno, M.C.M. FTIR quantitative analysis of calcium carbonate (calcite) and silica (quartz) mixtures using the constant ratio method. Application to geological samples. *Talanta* **2002**, *58*, 811–821. [CrossRef]
- 58. Čadež, V.; Šegota, S.; Sondi, I.; Lyons, D.M.; Saha, P.; Saha, N.; Sikirić, M.D. Calcium phosphate and calcium carbonate mineralization of bioinspired hydrogels based on β-chitin isolated from biomineral of the common cuttlefish (*Sepia officinalis*, L.). *J. Polym. Res.* 2018, 25, 226. [CrossRef]
- 59. Hossain, M.S.; Ahmed, S. FTIR spectrum analysis to predict the crystalline and amorphous phases of hydroxyapatite: A comparison of vibrational motion to reflection. *RSC Adv.* **2023**, *13*, 14625–14630. [CrossRef]
- 60. Lee, I.H.; Lee, J.A.; Lee, J.H.; Heo, Y.W.; Kim, J.J. Effects of pH and reaction temperature on hydroxyapatite powders synthesized by precipitation. *J. Korean Ceram. Soc.* **2020**, *57*, 56–64. [CrossRef]
- 61. Fleet, M.E.; Liu, X. Carbonate apatite type A synthesized at high pressure: New space group (P3) and orientation of channel carbonate ion. *J. Solid State Chem.* **2003**, 174, 412–417. [CrossRef]
- 62. Shiehpour, M.; Solgi, S.; Tafreshi, M.J.; Ghamsari, M.S. ZnO-doped KCl single crystal with enhanced UV emission lines. *Appl. Phys. A* **2019**, 125, 531. [CrossRef]
- 63. Chruszcz-Lipska, K.; Zelek-Pogudz, S.; Solecka, U.; Solecki, M.L.; Szostak, E.; Zborowski, K.K.; Zając, M. Use of the Far Infrared Spectroscopy for NaCl and KCl Minerals Characterization—A Case Study of Halides from Kłodawa in Poland. *Minerals* 2022, 12, 1561. [CrossRef]
- 64. Toshima, T.; Hamai, R.; Tafu, M.; Takemura, Y.; Fujita, S.; Chohji, T.; Tanda, S.; Li, S.; Qin, G.W. Morphology control of brushite prepared by aqueous solution synthesis. *J. Asian Ceram. Soc.* **2014**, *2*, 52–56. [CrossRef]
- 65. Niu, Y.Q.; Liu, J.H.; Aymonier, C.; Fermani, S.; Kralj, D.; Falini, G.; Zhou, C.H. Calcium carbonate: Controlled synthesis, surface functionalization, and nanostructured materials. *Chem. Soc. Rev.* **2022**, *51*, 7883–7943. [CrossRef] [PubMed]
- 66. Yelten-Yilmaz, A.; Yilmaz, S. Wet chemical precipitation synthesis of hydroxyapatite (HA) powders. *Ceram. Int.* **2018**, 44, 9703–9710. [CrossRef]

Compounds **2025**, 5, 41 22 of 23

67. Radulescu, D.-E.; Neacsu, I.A.; Grumezescu, A.-M.; Andronescu, E. Novel Trends into the Development of Natural Hydroxyapatite-Based Polymeric Composites for Bone Tissue Engineering. *Polymers* **2022**, *14*, 899. [CrossRef] [PubMed]

- 68. Fadeeva, I.V.; Deyneko, D.V.; Knotko, A.V.; Olkhov, A.A.; Slukin, P.V.; Davydova, G.A.; Trubitsyna, T.A.; Preobrazhenskiy, I.I.; Gosteva, A.N.; Antoniac, I.V.; et al. Antibacterial Composite Material Based on Polyhydroxybutyrate and Zn-Doped Brushite Cement. *Polymers* 2023, 15, 2106. [CrossRef]
- 69. del-Mazo-Barbara, L.; Gomez-Cuyas, J.; Martinez-Orozco, L.; Perez, O.S.; Bou-Petit, E.; Ginebra, M.P. In vitro degradation of 3D-printed polycaprolactone\biomimetic hydroxyapatite scaffolds: Impact of the sterilization method. *Polym. Test.* **2024**, 139, 108566. [CrossRef]
- 70. Mirkiani, S.; Mesgar, A.S.; Mohammadi, Z.; Matinfar, M. Synergetic reinforcement of brushite cements by monetite/apatite whisker-like fibers and carboxymethylcellulose. *Materialia* **2022**, *21*, 101329. [CrossRef]
- 71. Safronova, T.; Kiselev, A.; Selezneva, I.; Shatalova, T.; Lukina, Y.; Filippov, Y.; Toshev, O.; Tikhonova, S.; Antonova, O.; Knotko, A. Bioceramics Based on β-Calcium Pyrophosphate. *Materials* **2022**, *15*, 3105. [CrossRef]
- 72. Bolarinwa, A.; Gbureck, U.; Purnell, P.; Bold, M.; Grover, L.M. Cement casting of calcium pyrophosphate based bioceramics. *Adv. Appl. Ceram.* **2010**, *109*, 291–295. [CrossRef]
- 73. Saxena, A.; Vignesh, R.; Roy, S.; Sahai, S.; Bhattacharjee, D.; Basu, B.; Mukherjee, S. Synthesis and properties of tailored β-tricalcium phosphate for bone filler applications. *Int. J. Appl. Ceram. Technol.* **2025**, 22, e14957. [CrossRef]
- 74. Safronova, T.; Grigorev, G.; Shatalova, T.; Roslyakov, I.; Platonov, V.; Khayrutdinova, D. Microporous Ceramics Based on β-Tricalcium Phosphate. *Ceramics* **2022**, *5*, 1269–1285. [CrossRef]
- 75. Toshev, O.U.; Safronova, T.V.; Mironova, Y.S.; Matveeva, A.S.; Shatalova, T.B.; Filippov, Y.Y.; Knotko, A.V.; Akhmedov, M.R.; Kukueva, E.V.; Lukina, Y.S. Ultraporous submicron-grained β-Ca₃(PO₄)₂-based ceramics. *Inorg. Mater.* 2022, 58, 1208–1219. [CrossRef]
- 76. Martin, R.I.; Brown, P.W. Phase equilibria among acid calcium phosphates. J. Am. Ceram. Soc. 1997, 80, 1263–1266. [CrossRef]
- 77. Rasouli, M.; Darghiasi, S.F.; Naghib, S.M.; Rahmanian, M. Multifunctional hydroxyapatite-based nanoparticles for biomedicine: Recent progress in drug delivery and local controlled release. *Curr. Mech. Adv. Mater.* **2021**, *1*, 3–16. [CrossRef]
- 78. Ismail, R.; Cionita, T.; Shing, W.L.; Fitriyana, D.F.; Siregar, J.P.; Bayuseno, A.P.; Nugraha, F.W.; Muhamadin, R.C.; Junid, R.; Endot, N.A. Synthesis and Characterization of Calcium Carbonate Obtained from Green Mussel and Crab Shells as a Biomaterials Candidate. *Materials* 2022, 15, 5712. [CrossRef] [PubMed]
- 79. Dosen, A.; Giese, R.F. Thermal decomposition of brushite, CaHPO₄·2H₂O to monetite CaHPO₄ and the formation of an amorphous phase. *Am. Mineral.* **2011**, *96*, 368–373. [CrossRef]
- 80. Zhou, H.; Yang, L.; Gbureck, U.; Bhaduri, S.B.; Sikder, P. Monetite, an important calcium phosphate compound–Its synthesis, properties and applications in orthopedics. *Acta Biomater.* **2021**, *127*, 41–55. [CrossRef]
- 81. Griesiute, D.; Gaidukevic, J.; Zarkov, A.; Kareiva, A. Synthesis of β-Ca₂P₂O₇ as an Adsorbent for the Removal of Heavy Metals from Water. *Sustainability* **2021**, 13, 7859. [CrossRef]
- 82. El Hazzat, M.; El Hamidi, A.; Halim, M.; Arsalane, S. Complex evolution of phase during the thermal investigation of Brushite-type calcium phosphate CaHPO₄.2H₂O. *Materialia* **2021**, *16*, 101055. [CrossRef]
- 83. Babou-Kammoe, R.; Hamoudi, S.; Larachi, F.; Belkacemi, K. Synthesis of CaCO₃ nanoparticles by controlled precipitation of saturated carbonate and calcium nitrate aqueous solutions. *Can. J. Chem. Eng.* **2012**, *90*, 26–33. [CrossRef]
- 84. Rabinovich, V.A.; Khavin, Z.Y. A Short Chemical Reference Book; Chemistry: Leningrad, Russia, 1978; 392p. (In Russian)
- 85. Zhou, D.; Dong, J.; Si, Y.; Zhu, F.; Li, J. Melting Curve of Potassium Chloride from in situ Ionic Conduction Measurements. *Minerals* **2020**, *10*, 250. [CrossRef]
- 86. Cavalcante, L.d.A.; Ribeiro, L.S.; Takeno, M.L.; Aum, P.T.P.; Aum, Y.K.P.G.; Andrade, J.C.S. Chlorapatite Derived from Fish Scales. *Materials* **2020**, *13*, 1129. [CrossRef]
- 87. Bohner, M.; Santoni, B.L.G.; Döbelin, N. β-tricalcium phosphate for bone substitution: Synthesis and properties. *Acta Biomater*. **2020**, *113*, 23–41. [CrossRef]
- 88. Putlyaev, V.I.; Evdokimov, P.V.; Safronova, T.V.; Klimashina, E.S.; Orlov, N.K. Fabrication of osteoconductive Ca_{3-x} M_{2x} (PO₄)₂ (M = Na, K) calcium phosphate bioceramics by stereolithographic 3D printing. *Inorg. Mater.* **2017**, *53*, 529–535. [CrossRef]
- 89. Alaoui, Y.; El Moudane, M.; Er-rafai, A.; Khachani, M.; Ghanimi, A.; Sabbar, A.; Tabyaoui, M.; Guenbour, A.; Bellaouchou, A. Structural study, thermal and physical properties of K₂O-CaO-P₂O₅ phosphate glasses. *Moroc. J. Chem.* **2021**, *9*, 454–463. [CrossRef]
- 90. Wang, Y.H.; Chen, Y.J.; Geng, X.J.; Yang, Y.; Li, Z.Q.; Zuo, X.Y. Effect of heavy-doping Eu³⁺ and charge compensation on crystalline phase and luminescence properties of K₂CaP₂O₇ phosphors emitting orange-red light. *J. Chem. Sci.* **2024**, *136*, 16. [CrossRef]
- 91. Brown, E.H.; Lehr, J.R.; Frazier, A.W.; Smith, J.P. Fertilizer materials, calcium ammonium and calcium potassium pyrophosphate systems. *J. Agric. Food Chem.* **1964**, *12*, 70–73. [CrossRef]

Compounds 2025, 5, 41 23 of 23

92. Xu, S.; Duan, J.; Dong, P.; Wang, M.; Zhang, Y.; Yu, J. Highly dispersed Eu²⁺ activated Ca₁₀(PO₄)₆Cl₂ phosphor with enhanced blue emitting through deposition-precipitation process. *Opt. Mater.* **2020**, *110*, 110529. [CrossRef]

93. Kannan, S.; Rebelo, A.; Lemos, A.F.; Barba, A.; Ferreira, J.M.F. Synthesis and mechanical behaviour of chlorapatite and chlorapatite/β-TCP composites. *J. Eur. Ceram. Soc.* **2007**, 27, 2287–2294. [CrossRef]

Disclaimer/Publisher's Note: The statements, opinions and data contained in all publications are solely those of the individual author(s) and contributor(s) and not of MDPI and/or the editor(s). MDPI and/or the editor(s) disclaim responsibility for any injury to people or property resulting from any ideas, methods, instructions or products referred to in the content.